

## Metagenomic Mining for Esterases in the Microbial Community of Los Rueldos Acid Mine Drainage Formation

Vidal, Paula; Martinez-Martinez, Monica; Fernandez-Lopez, Laura; Roda, Sergio; Mendez-Garcia, Celia; Golyshina, Olga; Guallar, Victor; Pelaez, Ana I.; Ferrer, Manuel

**Frontiers in Microbiology**

DOI:  
[10.3389/fmicb.2022.868839](https://doi.org/10.3389/fmicb.2022.868839)

Published: 19/05/2022

Peer reviewed version

[Cyswllt i'r cyhoeddiad / Link to publication](#)

*Dyfyniad o'r fersiwn a gyhoeddwyd / Citation for published version (APA):*

Vidal, P., Martinez-Martinez, M., Fernandez-Lopez, L., Roda, S., Mendez-Garcia, C., Golyshina, O., Guallar, V., Pelaez, A. I., & Ferrer, M. (2022). Metagenomic Mining for Esterases in the Microbial Community of Los Rueldos Acid Mine Drainage Formation. *Frontiers in Microbiology*, 13. <https://doi.org/10.3389/fmicb.2022.868839>

### Hawliau Cyffredinol / General rights

Copyright and moral rights for the publications made accessible in the public portal are retained by the authors and/or other copyright owners and it is a condition of accessing publications that users recognise and abide by the legal requirements associated with these rights.

- Users may download and print one copy of any publication from the public portal for the purpose of private study or research.
- You may not further distribute the material or use it for any profit-making activity or commercial gain
- You may freely distribute the URL identifying the publication in the public portal ?

### Take down policy

If you believe that this document breaches copyright please contact us providing details, and we will remove access to the work immediately and investigate your claim.

# Metagenomic mining for esterases in the microbial community of Los Rueldos acid mine drainage formation

1 Paula Vidal<sup>1</sup>, Mónica Martínez-Martínez<sup>1,†</sup>, Laura Fernandez-Lopez<sup>1</sup>, Sergi Roda<sup>2</sup>, Celia  
2 Méndez-García<sup>3</sup>, Olga V. Golyshina<sup>4</sup>, Víctor Guallar<sup>2</sup>, Ana I. Peláez<sup>3</sup>, Manuel Ferrer<sup>1,\*</sup>

3 <sup>1</sup> Institute of Catalysis, Department of Applied Biocatalysis, Consejo Superior de Investigaciones  
4 Científicas, 28049 Madrid, Spain

5 <sup>2</sup> Department of Life Sciences, Barcelona Supercomputing Center and Institució Catalana de Recerca  
6 i Estudis Avançats, 08034 Barcelona, Spain

7 <sup>3</sup> Área de Microbiología, Departamento Biología Funcional e Instituto de Biotecnología de Asturias,  
8 Universidad de Oviedo, 33006 Oviedo, Asturias, Spain

9 <sup>4</sup> Centre for Environmental Biotechnology, School of Natural Sciences, Bangor University, LL57  
10 2UW Bangor, UK

11

## 12 †Current address

13 Facultad de Ciencias Biomédicas, Departamento de Ciencias de la Salud, Universidad Europea de  
14 Madrid, Urbanización El Bosque, Calle Tajo, s/n, 28670 Villaviciosa de Odón, Spain

15

## 16 \* Correspondence:

17 Corresponding Author

18 mferrer@icp.csic.es

19 **Keywords:** acidophiles, acidophilic bacteria, acid mine drainage, biodiversity, extremozymes,  
20 esterase, metagenomics, plastic.

## 21 Abstract

22 Acid mine drainage systems (AMDs) are extremely acidic and metal-rich formations inhabited by  
23 relatively low-complexity communities of acidophiles, whose enzymes remain mostly  
24 uncharacterized. Indeed, enzymes from only a few AMD sites have been studied. The low number of  
25 available cultured representatives and genome sequences of acidophiles inhabiting AMDs makes it  
26 difficult to assess the potential of these environments for enzyme bioprospecting. In this study, using  
27 naïve and in silico metagenomic approaches, we retrieved 16 esterases from the  $\alpha/\beta$ -hydrolase fold  
28 superfamily with the closest match from uncultured acidophilic *Acidobacteria*, *Actinobacteria*  
29 (*Acidithrix*, *Acidimicrobium*, and *Ferrimicrobium*), *Acidiphilium*, and other *Proteobacteria*  
30 inhabiting the Los Rueldos site, which is a unique AMD formation in northwestern Spain with a pH  
31 of ~2. Within this set, only two polypeptides showed high homology (99.4%), while for the rest, the  
32 pairwise identities ranged between 4 and 44.9%, suggesting that the diversity of active polypeptides  
33 was dominated not by a particular type of protein or highly similar clusters of proteins but by diverse  
34 nonredundant sequences. The enzymes exhibited amino acid sequence identities ranging from 39 to  
35 99% relative to homologous proteins in public databases, including those from other AMDs, thus  
36 indicating the potential novelty of proteins associated with a specialized acidophilic community. Ten  
37 of the 16 hydrolases were successfully expressed in *Escherichia coli*. The pH for optimal activity

38 ranged from 7.0 to 9.0, with the enzymes retaining 33-68% of their activities at pH 5.5, which was  
 39 consistent with the relative frequencies of acid residues (from 54 to 67%). The enzymes were the  
 40 most active at 30-65 °C, retaining 20-61% of their activity under the thermal conditions  
 41 characterizing Los Rueldos ( $13.8 \pm 0.6^\circ\text{C}$ ). The analysis of the substrate specificity revealed the  
 42 capacity of six hydrolases to efficiently degrade (up to  $1652 \pm 75$  U/g at pH 8.0 and  $30^\circ\text{C}$ ) acrylic-  
 43 and terephthalic-like (including bis(2-hydroxyethyl)-terephthalate, BHET) esters, and these enzymes  
 44 could potentially be of use for developing plastic degradation strategies yet to be explored. Our  
 45 assessment uncovers the novelty and potential biotechnological interest of enzymes present in the  
 46 microbial populations that inhibit the Los Rueldos AMD system.

## 47 1 Introduction

48 In biotechnology, there is high interest in finding enzymes with new or improved properties (Pellis et  
 49 al., 2017; Ferrer et al., 2019). This interest is especially increased in relation to enzymes from  
 50 extremophiles, which are microorganisms that have evolved to thrive in extreme environments  
 51 (Baweja et al., 2016), as they can operate efficiently under multiple conditions requested by industry.  
 52 One example application is the eco-friendly bioconversion of cellulosic biomass by extremozymes,  
 53 which produces green products and has less substrate loss (Thapa et al., 2020). Furthermore, plastic  
 54 disposal is one of the major problems currently faced by the environment, as enormous quantities of  
 55 synthetic plastics are nondegradable. Researchers are constantly exploring new ways to degrade  
 56 plastics, and one of these ways involves using enzymes from microorganisms or microbial  
 57 communities, including some that inhabit extreme environments (Nchedo Ariole and George-West,  
 58 2020).

59 Acid mine drainage (AMD) systems deserve special attention as a source of extremozymes.  
 60 AMDs are extremely acidic runoff formations that originate from the microbial oxidation of pyrite  
 61 and other sulfide minerals, which results in the production of sulfuric acid and metal-rich solutions  
 62 (Méndez-García et al., 2015; Johnson and Quatrini, 2020). AMD systems are common on our planet,  
 63 although only a limited number of them have been microbiologically characterized (Méndez-García  
 64 et al., 2015; Johnson and Quatrini, 2020). Although it has recently been demonstrated that some of  
 65 these AMD formations, such as the Los Rueldos mercury mine in northwestern Spain (Méndez-  
 66 García et al., 2014), appear to be populated by a great diversity of bacteria and archaea, the majority  
 67 of them are inhabited by a restricted set of acidophilic bacteria and archaea (Golyshina, 2011;  
 68 Dopson et al., 2014; Méndez-García et al., 2015; Chen et al., 2016; Johnson and Quatrini, 2020),  
 69 whose diversity and abundance depend on geochemical constraints (Méndez-García et al., 2014;  
 70 Méndez-García et al., 2015; Huang et al., 2016).

71 Major bacterial lineages detected in AMD systems include the phyla *Proteobacteria*  
 72 (*Acidithiobacillus*, *Acidiphilium*, *Acidocella*, *Acidicaldus*, *Acidomonas*, *Acidisphaera*, ‘*Ferrovum*’,  
 73 and *Acidibacter*, and *Metallibacterium* spp.), *Nitrospirae* (*Leptospirillum* spp. such as *L.*  
 74 *ferrooxidans*, *L. ferriphilum*, and ‘*L. ferrodiazotrophum*’), *Actinobacteria*, *Firmicutes* (*Sulfobacillus*  
 75 spp., and *Alicyclobacillus* spp.), *Acidobacteria*, *Saccharibacteria* (TM7) and other candidate phyla  
 76 radiation (CPR) organisms. Archaea include the phyla *Euryarchaeota* (*Ferroplasma* spp. such as *F.*  
 77 *acidiphilum* and ‘*F. acidarmanus*’, *Acidiplasma cupricumulans*, and *Cuniculiplasma divulgatum*) and  
 78 *Thaumarchaeota* and the Candidate divisions ‘*Micrarchaeota*’ and ‘*Parvarchaeota*’ (Baker et al.,  
 79 2006; Baker et al., 2010; Golyshina et al., 2000; Golyshina et al., 2009; Golyshina, 2011; Dopson et  
 80 al., 2014; Golyshina et al., 2016; Chen et al., 2016; Chen et al., 2018; Korzhenkov et al., 2019;  
 81 Gavrillov et al., 2019). These microorganisms are expected to be reservoirs of enzymes selected to  
 82 resist acidic harsh conditions (at least regarding those produced as extracellular products) (Sharma et

83 al., 2012), some of which might be of biotechnological relevance (Gomes et al., 2003; Adrio and  
84 Damian, 2014).

85 In this category, esterases and lipases from the  $\alpha/\beta$ -hydrolase fold superfamily are appropriate  
86 biocatalysts for use in a modern circular bioeconomy because of their abundance (at least one per  
87 genome; Ferrer et al., 2015); the extensive knowledge that has been accumulated after the analysis of  
88 the biochemical features, sequences and structures of more than 280,638 such proteins (Bauer et al.,  
89 2019); their ease of identification (multiple available screening methods; Reyes-Duarte et al., 2012);  
90 and their outstanding properties in terms of stability, reactivity, and scalability, which make them  
91 third-choice tools for the functionalization and modification of low-reactivity hydrocarbon-like  
92 blocks, oils and fats (Daiha et al., 2015). Genomics and metagenomics can potentially make  
93 accessible an enormous reserve of such important biocatalysts in organisms or microbial  
94 communities inhabiting any environment, including AMD systems. However, only 239 of the  
95 280,638 sequences available at the Lipase Engineering Database (Bauer et al., 2019) have been  
96 retrieved from cultured microorganisms (listed above) and uncultured microorganisms that are  
97 inhabitants of AMD systems, including *Alicyclobacillus* spp., 118 in total; *Sulfobacillus* spp., 53;  
98 *Acidobacteria*, 34; *Acidithiobacillus*, 13; *Leptospirillum*, 9; ‘*Ferrovum*’, 5; *Acidocella*, 3; and  
99 *Ferroplasma*, *Aciditrix* (1), *Acidiphilium*, and *Metallibacterium*, 1 each. Among these biocatalysts,  
100 only a low-pH optimum carboxylesterase from *F. acidiphilum* (Ohara et al., 2014) has been  
101 characterized. This limits the assessment of the biotechnological potential of acidophiles living in  
102 AMD systems, at least regarding esterases and lipases. The minimal enzyme-level information that is  
103 known about these systems is restricted to two endo-acting amylases with no similarity to any known  
104 protein and two genes conferring metal and acid resistance from the microbial community inhabiting  
105 the AMD systems of the Carnoulès (lead–zinc) mine in France (Delavat et al., 2012) and the Tinto  
106 River in southwestern Spain (Delavat et al., 2012; Guazzaroni et al., 2013), respectively.

107 To fill this knowledge gap, we initiated a metagenomic investigation to isolate carboxylesterases  
108 from a recently discovered and microbiologically characterized AMD formation, namely, the Los  
109 Rueldos mercury mine in northwestern Spain (Méndez-García et al., 2014). By applying homology  
110 searches in metagenomic sequences and naïve screening in clone libraries containing enzyme  
111 substrates, we discovered a number of such enzymes whose characteristics are reported herein. Both  
112 function- and DNA sequence-based metagenomic methods are complementary, with each having  
113 advantages and disadvantages. Bioinformatics methods allow a rapid process of enzyme searching;  
114 however, in prokaryotic genomes, >30% of genes remain annotated as “hypothetical, conserved  
115 hypothetical or with general prediction”, and large numbers of genes may have nonspecific  
116 annotations (such as putative hydrolases). The analysis of biochemical functions is likely to provide a  
117 superior approach to avoid this limitation, especially when screening novel enzymes. However, only  
118 a few hundred specific enzymatic assays exist, with a limited number of them applied in a high-  
119 throughput manner for the naïve screening of metagenomics libraries.

120 Although the in vivo roles and expression levels of the genes encoding the hydrolases presented  
121 in this study are unknown, their sequences and results of biochemical analyses shed new light on the  
122 enzymology of the microbial inhabitants of the Los Rueldos AMD formation, which have been  
123 neglected in enzyme prospecting.

## 124 2 Materials and Methods

### 125 2.1 General experimental procedures

126 The source and brand of each of the esters [purity  $\geq 99\%$ ] used in this study was Merck Life Science  
 127 S.L.U., Madrid, Spain. The oligonucleotides used for DNA amplification were synthesized by Sigma  
 128 Genosys, Ltd. (Pampisford, Cambs, UK). The *Escherichia coli* EPI-300-T1R strain used for  
 129 pCCFOS1 fosmid library construction and screening was from Epicentre Biotechnologies (Madison,  
 130 WI). The *E. coli* strain GigaSingles used for gene cloning, and *E. coli* strain BL21 (DE3) used for  
 131 gene expression were from Novagen (Darmstadt, Germany).

## 132 2.2 Sampling site and sample collection

133 The Los Ruedos gallery is located along the northwestern slope of the Morgao Valley (2 km  
 134 northeast of the town of Mieres and 20 km southeast of Oviedo, which is the capital city of Asturias  
 135 in northwestern Spain; 43°15'47"N, 5°46'9"W). It is a 70 m-long gallery with 10-30 cm depths in the  
 136 shallower areas and 40-70 cm depths in the deeper sections (Méndez-García et al., 2014).  
 137 Microorganisms are developed along the AMD system (pH  $\sim 2$ ), forming a bedded acidic biofilm  
 138 with uppermost oxic (B1A) and lowermost anoxic (B1B) strata. The DNA samples from B1A and  
 139 B1B (see below) samples collected and used in this study were the same as those in the previous  
 140 work (Méndez-García et al. 2014). Briefly, samples were collected in sterile 50 mL tubes at two  
 141 sampling sites determined by the presence of each different macroscopic microbial growth  
 142 morphology (B1A: up to 2 cm deep; B1B: from 2 to 15 cm deep) and kept on ice until nucleic acid  
 143 extraction was performed (within the following 2 h).

## 144 2.3 Nucleic acid extraction, preparation of pCCFOS1 libraries and naïve screening

145 The DNA samples from B1A and B1B were the same as those used in a previous work (Méndez-  
 146 García et al. 2014), which were obtained using the Power Soil DNA extraction kit (Cambio,  
 147 Cambridge, UK) according to the manufacturer's guidelines. Prior to clone library construction, the  
 148 metagenomics DNA was concentrated by first adding 50  $\mu$ l of 3 M sodium acetate solution to 50  $\mu$ l  
 149 DNA extract. Precipitation was conducted by the addition of 1.25 ml of ethanol and incubation at  
 150 room temperature for 10 sec. Precipitated DNA was pelleted by centrifugation at 20,000 g for 10  
 151 min. The resulting pellets were washed with 500  $\mu$ l of 70% (v/v) ethanol twice, and the traces of  
 152 ethanol were evaporated by incubation under a fume hood at room temperature for 10 min. The  
 153 resulting pellets were then dissolved in 20  $\mu$ l of sterile nuclease-free water. Before cloning in the  
 154 large-insert pCCFOS1 fosmid libraries using the CopyControl Fosmid Library Kit (Epicentre  
 155 Biotechnologies, Madison, USA) and the *E. coli* EPI300-T1<sup>R</sup> strain, the DNA (10  $\mu$ g) that was  
 156 unshered by gel electrophoresis was subjected to shearing by pipetting through a 200  $\mu$ l pipette tip  
 157 100 times, following the recommendations of the supplier (Epicentre Biotechnologies, Madison,  
 158 USA) to reach an approx. size of 30,000 bp. Cells of each pCCFOS1 fosmid library were suspended  
 159 in glycerol to a final concentration of 20% (v/v) and stored at  $-80^{\circ}\text{C}$  until further use. We generated  
 160 subsets of 94,000 and 81,000 clones for the B1A and B1B samples, respectively. Restriction analysis  
 161 of 10 randomly selected clones from each library revealed average insert sizes of 34,000 bp (for the  
 162 B1A samples) and 39,500 bp (for the B1B samples), which included nearly 3.2 Gbp of community  
 163 genomes per sample. This size is within the range of the average size range of DNA inserts in  
 164 positive clones found in this study (see below).

165 Fosmid clones were plated onto large (22.5 x 22.5 cm) Petri plates with Luria Bertani (LB) agar  
 166 containing chloramphenicol (12.5  $\mu$ g/ml) and induction solution (Epicentre Biotechnologies; WI,  
 167 USA) at a quantity recommended by the supplier to induce a high fosmid copy number. Clones were  
 168 scored by the ability to hydrolyze  $\alpha$ -naphthyl acetate ( $\alpha$ -NA) and tributyrin, as previously described  
 169 (Reyes-Duarte et al., 2012). Positive clones presumptively containing carboxylesterases and lipases

170 with the  $\alpha/\beta$  hydrolase fold were selected, and their DNA inserts were sequenced using a MiSeq  
171 Sequencing System (Illumina, San Diego, USA) with a  $2 \times 150$ -bp sequencing v2 kit at  
172 Lifesequencing S.L. (Valencia, Spain). Before sequencing fosmid DNA was extracted from the  
173 fosmid clones containing the metagenomic segments using the QUIAGEN Large-Construct Kit  
174 (QUIAGEN, Hilden, Germany), according to the manufacturer's protocol. Upon the completion of  
175 sequencing, the reads were quality-filtered and assembled to generate nonredundant meta-sequences,  
176 and genes were predicted and annotated as described previously (Placido et al., 2015).

## 177 **2.4 Selection of genes encoding enzymes by homology sequence analysis**

178 The predicted protein-coding genes obtained in a previous study (Méndez-García et al., 2014) after  
179 the sequencing of DNA material from resident microbial communities in each of the samples (B1A  
180 and B1B) with a Roche 454 GS FLX Ti sequencer (Roche Applied Science, Penzberg, Germany)  
181 were used in this study. The meta-sequences are available from the National Center for  
182 Biotechnology Information (NCBI) nonredundant public database with the IDs PRJNA193663 (for  
183 B1A) and PRJNA193664 (for B1B). Protein-coding genes identified from metagenomes (sequence-  
184 based screening) and from the DNA inserts of positive clones (naïve screen) were screened (score  $>$   
185 45; e-value  $< 10e^{-3}$ ) using BLASTP and PSI-BLAST searching (Altschul et al., 1997) for enzymes of  
186 interest against the ESTHER (*ESTerases and alpha/beta-Hydrolase Enzymes and Relatives*) and  
187 LED (*Lipase Engineering*) databases (Fischer and Pliess, 2003; Barth et al., 2004).

## 188 **2.5 Gene expression and protein purification**

189 The experimental procedures used for the cloning, expression, and purification of selected proteins  
190 (either from naïve or homology sequence screening) in the Ek/LIC 46 vector and *E. coli* strain BL21  
191 (DE3) were performed as described previously (Alcaide et al., 2015). The primers used for  
192 amplification are listed in the Supplementary Methods. All proteins studied here were N-terminally  
193 His<sub>6</sub>-tagged, and the soluble His-tagged proteins were produced and purified at room temperature  
194 after binding to a nickel–nitrilotriacetic acid (Ni–NTA) His-Bind resin (from Merck Life Science  
195 S.L.U., Madrid, Spain) as described previously (Giunta et al., 2020), with slight modifications (the  
196 expression culture was scaled up to 1 L using 50 ml preinoculum). The purity was assessed as  $>98$  %  
197 using SDS–PAGE (**Supplementary Figure 1**) in a Bio-Rad Mini Protein system (Laemmli, 1970).  
198 Protein concentrations were determined according to the Bradford method with bovine serum  
199 albumin as the standard (Bradford, 1976). A total of approximately 0.8 to 37 mg of purified  
200 recombinant proteins was obtained from each 1 L culture on average, as follows: Est<sub>A1</sub> (6.4 mg/l),  
201 Est<sub>A2</sub> (25 mg/l), Est<sub>A3</sub> (13 mg/l), Est<sub>A4</sub> (37 mg/l), Est<sub>A5</sub> (41 mg/l), Est<sub>A6</sub> (7 mg/l), Est<sub>A7</sub> (0.8 mg/l),  
202 Est<sub>A8</sub> (19 mg/l), Est<sub>B1</sub> (1.0 mg/l), and Est<sub>B2</sub> (32 mg/l).

## 203 **2.6 Enzyme assays**

204 The hydrolysis of 2-naphthyl acrylate (ref. 577189), tri(propylene glycol) diacrylate (ref. 246832),  
205 dibenzyl terephthalate (ref. PH000126) and bis(2-hydroxyethyl)-terephthalate (BHET; ref. 465151)  
206 (all from Merck Life Science S.L.U., Madrid, Spain) was assessed using a pH indicator assay in 384-  
207 well plates (ref. 781162, Greiner Bio-One GmbH, Kremsmünster, Austria) at 30°C and pH 8.0 in a  
208 Synergy HT Multi-Mode Microplate Reader in continuous mode at 550 nm over 24 h (extinction  
209 coefficient ( $\epsilon$ ) of phenol red, 8450 M<sup>-1</sup>cm<sup>-1</sup>). The acid produced after ester bond cleavage by the  
210 hydrolytic enzyme induced a color change in the pH indicator that was measured  
211 spectrophotometrically at 550 nm. The experimental conditions were as detailed previously (Giunta  
212 et al., 2020), with the absence of activity defined as at least a twofold background signal. For  $V_{\max}$   
213 determination, [protein]: 270  $\mu$ g/ml; [ester]: 20 mM; reaction volume: 44  $\mu$ l; T: 30°C; and pH: 8.0.

214 Activity was calculated by determining the absorbance per minute from the generated slopes and  
 215 applying the following formula:

$$216 \quad \text{Rate} \left( \frac{\mu\text{mol}}{\text{min mg protein}} \right) = \frac{\frac{\Delta\text{Abs}}{\text{min}}}{8450 \text{ M} - 1\text{cm} - 1} * \frac{1}{0.4 \text{ cm}} * \frac{10^6 \mu\text{M}}{1 \text{ M}} * 0.000044 \text{ L} * \frac{1}{\text{mg prot.}}$$

217

218 The activity toward the model esters *p*-nitrophenyl acetate (*pNPC*<sub>2</sub>), propionate (*pNPC*<sub>3</sub>), butyrate  
 219 (*pNPC*<sub>4</sub>), octanoate (*pNPC*<sub>8</sub>), decanoate (*pNPC*<sub>10</sub>) and decanoate (*pNPC*<sub>12</sub>) was assessed in 50 mM  
 220 Britton and Robinson (BR) buffer at pH 8.0 and 30°C by monitoring the production of 4-nitrophenol  
 221 at 348 nm (pH-independent isosbestic point,  $\epsilon = 4147 \text{ M}^{-1} \text{ cm}^{-1}$ ) over 5 min and determining the  
 222 absorbance per minute from the generated slopes (Santiago et al., 2018). The reactions were  
 223 performed at 30°C in 96-well plates (ref. 655801, Greiner Bio-One GmbH, Kremsmünster, Austria)  
 224 and contained 0.09 to 3  $\mu\text{g}$  proteins and 0.8 mM esters in a total volume of 200  $\mu\text{l}$ . The effect of pH  
 225 on the activity was determined in 50 mM BR buffer at pH 4.0–12.0, as described previously. Similar  
 226 assay conditions were used to assay the effects of temperature on the ester hydrolysis of *pNPC*<sub>3</sub>, but  
 227 in this case, the reactions were performed in 50 mM Britton and Robinson buffer pH 7.0. Note that  
 228 the BR buffer consists of a mixture of 0.04 M  $\text{H}_3\text{BO}_3$ , 0.04 M  $\text{H}_3\text{PO}_4$  and 0.04 M  $\text{CH}_3\text{COOH}$  that has  
 229 been titrated to the desired pH with 0.2 M NaOH. All values were determined in triplicate and were  
 230 corrected for nonenzymatic transformation. In all cases, the activity was calculated by determining  
 231 the absorbance per minute from the generated slopes and applying the following formula:

$$232 \quad \text{Rate} \left( \frac{\mu\text{mol}}{\text{min mg protein}} \right) = \frac{\frac{\Delta\text{Abs}}{\text{min}}}{4147 \text{ M} - 1\text{cm} - 1} * \frac{1}{0.4 \text{ cm}} * \frac{10^6 \mu\text{M}}{1 \text{ M}} * 0.0002 \text{ L} * \frac{1}{\text{mg protein}}$$

233

234 Poly(propylene glycol) diacrylate (ref. 455024, Merck Life Science S.L.U., Madrid, Spain) and  
 235 poly(DL-lactide) with an average molecular weight 2000 (ref. AP224, PolySciTech, Akina, IN,  
 236 USA) were assayed as described previously (Hajighasemi et al., 2018). The hydrolysis of  
 237 polyethylene terephthalate (PET) films (prepared as reported by Bollinger et al., 2020) and particles,  
 238 which were prepared using PET from a bottle (from a local shop – Granini brand) as described  
 239 previously (Pütz et al., 2006), was evaluated at 30°C and pH 8.0 with 270  $\mu\text{g}$  protein/ml, and 2 mg/  
 240 ml plastic material, as previously reported (Bollinger et al., 2020).

241 The effect of the inhibitors mercaptoethanol (ref. M7154) and iodoacetamide (ref. I1149), which  
 242 were both from Merck Life Science S.L.U., Madrid, Spain, was tested as follows. A mixture  
 243 containing the purified enzymes (final concentration of 1 mg/ml) in 190  $\mu\text{l}$  of 40 mM 4-(2-  
 244 hydroxyethyl)-1-piperazineethanesulfonic acid (HEPES) at pH 7.0 and the inhibitors (final  
 245 concentration, 1-10 mM) was incubated for 5 min to 24 h at 30-45°C. The reaction was initiated by  
 246 adding *pNPC*<sub>3</sub> (0.8 mM, final concentration), and the activity was measured over 5 min as described  
 247 above and compared to control samples without inhibitors.

## 248 2.7 Circular dichroism (CD) to estimate thermal denaturation

249 CD spectra were acquired between 190 and 270 nm with a Jasco J-720 spectropolarimeter equipped  
 250 with a Peltier temperature controller in a 0.1-mm cell at 25°C. The spectra were analyzed, and  
 251 denaturation temperature (*T*<sub>d</sub>) values were determined at 220 nm between 10 and 85°C at a rate of  
 252 30°C per hour in 40 mM HEPES buffer at pH 7.0. CD measurements were performed at pH 7.0 and

253 not at the optimal pH (8.5-9.0) to ensure protein stability. A protein concentration of 0.5 mg/ml was  
 254 used.  $T_d$  (and the standard deviation of the linear fit) was calculated by fitting the ellipticity (mdeg) at  
 255 220 nm at each of the different temperatures using a 5-parameter sigmoid fit with SigmaPlot 13.0.

## 256 **2.8 Codes and accession numbers**

257 The sequences were named based on the code 'Est', which refers to Esterase, followed by a letter  
 258 indicating the origin of the sample, as follows: Est<sub>A</sub>, esterase from the uppermost oxic B1A strata,  
 259 and Est<sub>B</sub>, esterase from the lowermost anoxic B1B sediment attached strata. The final number  
 260 (subscript) is an arbitrary number representing the number of enzymes per site. Sequences encoding  
 261 enzymes were deposited under the BioProject IDs PRJNA193663 (for B1A) and PRJNA193664 (for  
 262 B1B) in the NCBI public database, with the accession numbers detailed in **Table 1**.

## 263 **2.9 3D modeling**

264 The models of the protein structures were predicted with AlphaFold 2.1.0 (Jumper et al., 2021).

## 265 **3 Results**

### 266 **3.1 Enzyme selection and divergence at the sequence level**

267 Microbial communities inhabiting two distinct compartments within Los Ruedos AMD  
 268 formation were screened for sequences encoding carboxylesterases or lipases. For that we used two  
 269 complementary metagenomics approaches, namely, naïve and homology sequence screens. First, a  
 270 total of approximately 81,000 pCCFOS1 clones from each clone library (approximately 2.8 Gbp for  
 271 B1A and 3.20 Gbp for B1B) were screened for esterase/lipase activity using plate-based screen with  
 272  $\alpha$ NA and tributyrin as model substrates. We identified a total of 10 positive clones being active  
 273 against both substrates in the B1A clone library, whereas no positives were found in the B1B library.  
 274 The fosmids with insert lengths ranging from 16,545 to 41,280 bp were fully sequenced, from which  
 275 10 genes (one per positive clone) encoding presumptive esterases/lipases were identified. In addition,  
 276 we searched the predicted protein-coding genes obtained through next-generation sequencing for  
 277 sequences encoding esterases and lipases by BLAST search against the ESTHER (*ESTerases and*  
 278 *alpha/beta-Hydrolase Enzymes and Relatives*) and LED (*Lipase Engineering*) databases (43, 44). A  
 279 total of 6 full-length sequences (B1A: 2; B1B: 4), with accession numbers EQD63018.1,  
 280 EQD66234.1, EQD71191.1, EQD52136.1, EQD55146.1 and EQD26916.1, encoding potential  
 281 enzymes were identified. Taken together, a total of 16 genes encoding hydrolases from the  $\alpha/\beta$ -  
 282 hydrolase fold superfamily, specifically, 12 from B1A (EstA<sub>1</sub> to EstA<sub>12</sub>) and 4 from B1B (EstB<sub>1</sub> to  
 283 EstB<sub>4</sub>), were identified (**Table 1**). As determined by Matcher (EMBOSS package), the pairwise  
 284 amino acid sequence identity for 14 of the 16  $\alpha/\beta$  hydrolases ranged from 4.0 to 44.9%. This,  
 285 together with the fact that only 2 out of 16 polypeptides were highly similar (EstA<sub>5</sub> and EstA<sub>6</sub> differ  
 286 in only 2 amino acids: arginine 152 and alanine 179 in EstA<sub>5</sub> are cysteine 152 and threonine 179 in  
 287 EstA<sub>6</sub>), suggests a large divergence at the sequence level within the enzymes examined, and that the  
 288 diversity of polypeptides was not dominated by a particular type of protein or highly similar clusters  
 289 of proteins but rather by diverse nonredundant sequences. Note that only 1 of 10 sequences selected  
 290 after naïve screens was found in the metagenomic data generated after direct DNA sequencing  
 291 (EstA<sub>11</sub>, which is 99% identical to GenBank acc. nr. EQD37671.1 from the Los Ruedos metagenome  
 292 (Méndez-García et al., 2014)). This demonstrates that both types of screens (naïve and in silico) are  
 293 complementary tools for enzyme discovery. However, deeper metagenomic sequencing could  
 294 potentially detect all enzymes isolated by naïve screens.



295 The deduced molecular mass and estimated isoelectric point ( $pI$ ) values ranged from 23.19 to  
 296 101.53 kDa and from 4.62 to 10.04, respectively. Putative proteins exhibited a maximum amino acid  
 297 sequence identity ranging from 39 to 100% to putative esterases/lipases in public databases (Table 1).  
 298 It is worth mentioning that EstA<sub>3</sub>, EstA<sub>8</sub> and EstB<sub>3</sub> are related to presumptive esterase/lipase-like  
 299 subfamily proteins of the SGNH hydrolases, EstA<sub>11</sub> to presumptive glycoside-hydrolase family  
 300 GH114 (N-terminal domain) and CE4\_PelA\_like hydrolases (C-terminal domain), and EstA<sub>12</sub> to  
 301 presumptive sialate O-acetyl esterases. A further TBLASTX search against metagenomics proteins  
 302 deposited in databases revealed no similarity of 10 proteins with homologous acid mine drainage  
 303 metagenome proteins. In contrast, 5 proteins (EstA<sub>3</sub> to EstA<sub>6</sub>, and EstA<sub>12</sub>) do share from 27 to 54%  
 304 homology to 3 proteins from the Carnoules arsenic-contaminated mine drainage (GenBank:  
 305 CBI07622.1, CBH97521.1 and CBI00527.1). This finding suggests that esterases/lipases from  
 306 microbial communities from the Los Ruedos site are distantly related to proteins from other known  
 307 homologous proteins from AMD formations with metagenome sequences available. It also reflects  
 308 the large undiscovered pool of enzymes from bacterial species populating the Los Ruedos site.

### 309 3.2 Primary structure analysis

310 Based on the comparison of the primary structures, 14 families of sequence-related esterases and  
 311 lipases have been reported (Arpigny and Jaeger, 1999; Rao et al., 2013). Sequence analysis  
 312 categorized 13 enzymes from Los Ruedos into some of these known subfamilies (**Figure 1**) with  
 313 most structurally similar homologs as follows: EstA<sub>9</sub> (27%; best hit in Protein Data Bank (PDB)  
 314 3DOH\_A) and EstB<sub>4</sub> (41%; 3OM8\_A) to Family I; EstA<sub>1</sub> (41%; 3V9A\_A), EstA<sub>4</sub> (41%; 4YPV\_A),  
 315 EstA<sub>5</sub> (49%; 4YPV\_A) and EstA<sub>6</sub> (49%; 4YPV\_A) to Family IV; EstA<sub>7</sub> (53%; 4YPV\_A) and EstB<sub>2</sub>  
 316 (41%; 1AUO\_A) to Family VI; EstA<sub>2</sub> (37%; 2OGT\_A) to Family VII (EstA<sub>2</sub>); and EstA<sub>10</sub> (41%;  
 317 4IVK\_A) to beta-lactamase like Family VIII. EstA<sub>3</sub> (43%; PDB code 3P94\_A), EstA<sub>8</sub> (44%; PDB  
 318 code 3P94\_A) and EstB<sub>3</sub> (26%; PDB code 3KVN\_X) belong to Family II GDSL, but the structural  
 319 alignment also confirms that they contain a domain that displays the characteristic  $\alpha$ - $\beta$ - $\alpha$  globular  
 320 fold of the SGNH hydrolase family; EstB<sub>3</sub> also contains a passenger domain providing the driving  
 321 force for passenger translocation (Van de Berg, 2010). Three of the sequences could not be assigned  
 322 to these subfamilies. First, EstA<sub>11</sub> contains a 300 amino acid long N-terminal domain most similar to  
 323 glycoside-hydrolase family 114 and a 616 amino acid long C-terminal domain most similar to the  
 324 carbohydrate esterase 4 (CE4) superfamily that includes chitin deacetylases (EC 3.5.1.41), N-  
 325 acetylglucosamine deacetylases (EC 3.5.1.-), and acetylxylan esterases (EC 3.1.1.72), which catalyze  
 326 the N- or O-deacetylation of substrates such as acetylated chitin, peptidoglycan, and acetylated xylan.  
 327 Its N-terminal domain is structurally most similar (26%) to that of the glycosidase 2AAM\_A and its  
 328 C-terminal domain is structurally similar to the polysaccharide deacetylase from *Bacillus cereus*  
 329 (4HD5). Second, EstA<sub>12</sub> is associated with acetylxylan esterases (EC 3.1.1.72), with most similar  
 330 (21%) structural homolog in PDB being 1ZMB\_A. Third, EstB<sub>1</sub> shows homology to small serine  
 331 alpha/beta-hydrolase/acyl-peptidase (58%; 2FUK\_A). The tentative amino acids participating in the  
 332 typical catalytic triad of esterases and lipases are summarized in **Table 1**. Together, the analysis of  
 333 the primary sequence suggests that the diversity of esterases was not dominated by a particular type  
 334 of protein or highly similar clusters of proteins but rather by diverse nonredundant sequences  
 335 belonging to different microbial groups and distinct esterase/lipase subfamilies.

### 336 3.3 Source organisms of selected polypeptides

337 A search of oligonucleotide patterns against the GOHTAM database (Ménigaud et al., 2012) and  
 338 TBLASTX analysis revealed compositional similarities between the DNA fragment containing the  
 339 genes for EstA<sub>1</sub>, EstA<sub>2</sub>, EstA<sub>10</sub>, and EstB<sub>4</sub>, with genomic sequences of bacteria from the phylum

340 *Actinomycetota*. Among them, only unambiguous affiliations at lower levels could be achieved for  
 341 fragments containing EstA<sub>1</sub>, EstA<sub>2</sub> and EstA<sub>10</sub> that may most likely belong to bacteria from the genera  
 342 *Acidithrix* (EstA<sub>1</sub> and EstA<sub>10</sub>) and *Acidimicrobium/Ferrimicrobium* (EstA<sub>2</sub>), both from the family  
 343 *Acidimicrobiaceae* within the order *Acidimicrobiales*. Note that EstA<sub>1</sub> and EstA<sub>10</sub> showed 99-100%  
 344 sequence identity with uncharacterized esterases and lipases (WP\_052605564.1 and  
 345 WP\_052605292.1) from *Acidithrix ferrooxidans*, and EstA<sub>2</sub> showed 94% sequence identity with an  
 346 uncharacterized esterase-lipase (NNN14078.1) from *Acidimicrobiaceae*. EstA<sub>3</sub> was most likely  
 347 derived from an uncultured bacterium assigned to the phylum *Acidobacteria* with ambiguous  
 348 affiliation below the phylum level. The genes for EstA<sub>4</sub> to EstA<sub>9</sub>, EstA<sub>11</sub>, and EstB<sub>1</sub> to EstB<sub>3</sub> were  
 349 associated with uncultured bacteria of the *Proteobacteria* phylum, with ambiguous affiliations at a  
 350 lower taxonomic level, except for EstA<sub>4</sub>, which was most likely derived from a bacterium of the  
 351 genus *Acidiphilium* from the family *Acetobacteraceae* within the order *Rhodospirillales* (best hit  
 352 OYV70855.1 from *Acidiphilium* sp., 79% homology). All these bacterial groups have been detected  
 353 in biofilms thriving in the Los Ruedos mine (Méndez-García et al., 2014). No clear affiliation, other  
 354 than Bacteria, could be found for EstA<sub>12</sub>. Note, that in some cases no clear affiliation to a taxon of  
 355 source organism below the level of the phylum could be established, either because of the short  
 356 fragment length or the low compositional similarity between the metagenomic fragments and the  
 357 sequences of related bacterial chromosomes and plasmids do not allow proper assignments.

### 358 3.4 Enzyme characterization

359 From the 16 sequences selected, 8 from B1A and 2 from B1B were successfully cloned, expressed  
 360 and purified as soluble active proteins when expressed in pET Ek/LIC 46 vector and *E. coli* BL21 as  
 361 the host. These proteins were herein referred to as EstA<sub>1</sub> to EstA<sub>8</sub>, EstB<sub>1</sub> and EstB<sub>2</sub>. The remaining  
 362 six (EstA<sub>9</sub>-EstA<sub>12</sub> and EstB<sub>3</sub>-EstB<sub>4</sub>) could not be produced in soluble active form (they formed  
 363 inclusion bodies) in the expression system applied herein, which consists of the use of the IPTG-  
 364 inducible Ek/LIC 46 vector and *E. coli* strain BL21 (DE3) as a host, and their properties are not  
 365 described herein. Refining the expression conditions, which included variations in the expression  
 366 conditions (16, 30 and 37°C) and IPTG concentration (from 0.1 to 2 mM), resulted in unsuccessful  
 367 production of sufficient active protein material for characterization. Further efforts may be needed  
 368 with different expression vectors, which is beyond the scope of the present study.

369 The substrate profile of all  $\alpha/\beta$  hydrolases was first examined using a set of esters commonly  
 370 used to characterize esterases and lipases, namely, *p*NP esters such as *p*NPC<sub>2</sub>, *p*NPC<sub>3</sub>, *p*NPC<sub>4</sub>,  
 371 *p*NPC<sub>8</sub>, *p*NPC<sub>10</sub>, and *p*NPC<sub>12</sub>. All ester hydrolases preferred short-chain-length *p*NP-esters,  
 372 particularly *p*NPC<sub>2</sub> (EstA<sub>3</sub>), *p*NPC<sub>3</sub> (EstA<sub>2</sub>, EstA<sub>4</sub>, EstA<sub>5</sub>, EstA<sub>6</sub>, EstB<sub>1</sub> and EstB<sub>2</sub>) and *p*NPC<sub>4</sub> (EstA<sub>1</sub>,  
 373 EstA<sub>7</sub> and EstA<sub>8</sub>) (**Table 2**). Within all six *p*NP ester tested, all but one (EstA<sub>3</sub>) enzymes were able to  
 374 hydrolyze up to *p*NPC<sub>12</sub>, albeit at a much lower level (from 62- to 3,900-fold) compared to shorter  
 375 derivatives. Considering the preferred *p*NP esters, the maximum specific activity ranged from  
 376  $3.06 \pm 0.03$  to  $679.8 \pm 9.8$  units/mg. We further test the possibility that the enzymes hydrolyze  
 377 substrates other than *p*NP esters, particularly, plastic substrates and esters relevant to plastics. Using  
 378 previously described conditions (Hajighasemi et al., 2018; Bollinger et al., 2020), we did not find that  
 379 any of the enzymes hydrolyzed large plastic materials such as poly(propylene glycol) diacrylate,  
 380 poly(DL-lactide), amorphous PET film and PET nanoparticles. However, by using a pH-indicator  
 381 assay, we found that the enzymes were able to hydrolyze other terephthalate esters as well as acrylate  
 382 esters. Thus, as shown in **Table 3**, six of the enzymes hydrolyzed esters relevant to acrylic acid  
 383 plastics, e.g. 2-naphthyl acrylate and tripropylene glycol diacrylate, a commonly used material  
 384 principally exploited to prepare thermally stable polymers (He et al., 2017). These substrates, herein  
 385 found to be converted at a maximum rate of  $3,915 \pm 48$  units/g, are rarely hydrolyzed by esterases

386 and lipases, with only two examples reported, human salivary pseudocholinesterase and cholesterol  
 387 esterase (Finer et al., 2004; Cai et al., 2014). In addition, one of the enzymes (Est<sub>A8</sub>) was capable of  
 388 hydrolyzing dibenzyl terephthalate ( $432.2 \pm 27.5$  units/g), an intermediate produced during chemical  
 389 PET recycling with benzyl alcohol in the presence of a catalyst (Donahue et al., 2003). No esterase or  
 390 lipase has been reported to date that degrades this substrate. In addition, six of the esterases (Est<sub>A1</sub>,  
 391 Est<sub>A2</sub>, Est<sub>A5</sub>, Est<sub>A6</sub>, and Est<sub>A8</sub> and Est<sub>B2</sub>) efficiently hydrolyzed BHET (from  $5.0 \pm 1.0$  to  $336.9 \pm 3.6$   
 392 units/g), an intermediate in the degradation of PET (Yoshida et al., 2016); HPLC analysis, performed  
 393 as described (Bollinger et al., 2020), confirmed the hydrolysis of BHET to mono-(2-hydroxyethyl)-  
 394 terephthalic acid (MHET) and not to terephthalic acid. To conclude, the enzymes reported herein  
 395 from the Los Ruedos AMD formation showed high activity for converting and recycling  
 396 components of synthetic plastics, namely, acrylic- and terephthalate-based plastics, and could be of  
 397 potential use in developing plastic degradation strategies.

398 Using *pPNC*<sub>3</sub> as a substrate, the purified proteins were most active at temperatures ranging from  
 399 30 to 65 °C (**Figure 2**). The average annual temperature in Los Ruedos is  $13.8 \pm 0.6$  °C, which  
 400 varied from  $10 \pm 0.6$  °C to  $17.1 \pm 0.6$  (Méndez-García et al., 2014), with a temperature of 17 °C when  
 401 samples were taken (July). At this value, the enzymes retained 20 to 61% of the activity shown at the  
 402 optimal temperature (**Figure 2**).

403 Using *pPNC*<sub>3</sub> as a substrate, all enzymes showed an optimum pH for activity from neutral to  
 404 slightly basic, which varied from 7.0 to 9.0 (**Figure 2**). This finding suggests that these proteins are  
 405 most likely intracellularly produced, consistent with the absence of signal peptides in their sequences.  
 406 Even though the enzymes showed a slightly basic optimum pH, all retained 33 to 68% of their  
 407 activity at pH 5.5. Interestingly, Est<sub>A6</sub> shows two activity peaks, one at pH 5.5 and one at pH 9.0,  
 408 while Est<sub>A5</sub>, which only differs in two amino acids, has an optimum pH of 9.0 (**Figure 2**).

409 Sequence analysis revealed that Est<sub>A5</sub> and Est<sub>A6</sub> which have their origins in a bacterium of the  
 410 phylum *Proteobacteria*, differ in only 2 amino acids (99.4% identity). Positions 152 and 172 are  
 411 occupied by Arg and Ala in Est<sub>A5</sub> and by Cys and Thr in Est<sub>A6</sub>, respectively. Notably, Est<sub>A5</sub> was  
 412 most active at 30 °C, retaining more than 80% of the activity at temperatures from 20 to 45 °C  
 413 (**Figure 2**). The optimum temperature for activity increased up to 45 °C for Est<sub>A6</sub>, which maintained  
 414 more than 80% of its activity in the range from 30 to 60 °C. Analysis by circular dichroism revealed  
 415 that Est<sub>A5</sub> showed a sigmoidal curve from which a temperature of denaturation of  $60.4 \pm 0.2$  °C could  
 416 be obtained (**Figure 3**). However, the curve for Est<sub>A6</sub> shows two transitions, one with a denaturation  
 417 temperature of  $48.1 \pm 0.8$  °C, and a second at  $75.7 \pm 0.2$  °C. The presence of these two phases may  
 418 therefore indicate that the presence of these two amino acids may contribute to protein stability and  
 419 its denaturation under distinct conditions. This result may explain the higher optimum temperature  
 420 for the activity of this enzyme compared to Est<sub>A5</sub>, and the stabilization effect of Cys152 and Thr172.  
 421 This difference in thermostability between Est<sub>A5</sub> and Est<sub>A6</sub> can probably be explained by the  
 422 difference in amino acid 152, since Est<sub>A6</sub> has a Cys that would allow it to make a possible disulfide  
 423 bridge with Cys181, giving it greater thermostability than Est<sub>A5</sub> (since Est<sub>A5</sub> has an Arg at position  
 424 152 instead of a Cys), as shown by examination of the 3D models (**Supplementary Figure 2, Figure**  
 425 **4**). It is plausible that this difference may also be responsible for the different pH profiles of both  
 426 enzymes (**Figure 2**). If the disulfide bridge was present in Est<sub>A6</sub>, it could be removed by reduction or  
 427 chemical modification. Activity tests revealed that both enzymes are resistant to the reducing agent  
 428 beta-mercaptoethanol, with no activity lost even after 24 h of incubation at 30-45 °C in the presence  
 429 of 1-10 mM inhibitor. By contrast, in the presence of the cysteine alkylating agent iodoacetamide,  
 430 both enzymes were rapidly inactivated after 5 min. Thus we could not verify the presumptive  
 431 formation of the disulfide bridge in Est<sub>A6</sub> and further studies are needed to test this assumption.

432 **4 Discussion**

433 The effects of environmental constraints as prime forces shaping acid mine drainage populations  
434 have only begun to be elucidated through omics studies (Méndez-García et al., 2015). These effects  
435 are also of high interest in the context of the isolation and characterization of novel enzymes, for  
436 which limited data are available. However, the difficulty of cultivating organisms inhabiting AMD  
437 sites, which is due to their longer generation times, lower biomass yields and cultivation conditions  
438 that are not yet fully understood, requires different strategies to overcome the problems associated  
439 not only with their cultivation but also with the isolation of enzymes. Metagenomic approaches allow  
440 the screening of enzymes from such extreme environments. However, by using these tools, we have  
441 thus far explored only a small fraction of the enormous diversity on the planet, especially that of  
442 organisms inhabiting extremely acidic environments (Ferrer et al., 2015), again indicating the  
443 importance of establishing enzyme screening programs for AMD sites. The particular characteristics  
444 of the Los Ruedos AMD site (Méndez-García et al., 2015) that make it an interesting study site  
445 include the following. First, it is populated by a larger diversity of *Bacteria* and *Archaea* compared to  
446 other AMD sites, containing a total of 39 different species. Second, it has high microbial  
447 heterogeneity in local microniches defined by its O<sub>2</sub> concentration gradients and spatial and biofilm  
448 architecture. As an example, only 1 of 18 species inhabiting the two distinct compartments in a  
449 stratified streamer investigated herein, namely, the oxic uppermost (B1A) and anoxic lowermost  
450 (B1B) sediment-attached strata, was shared. Therefore, it is plausible that Los Ruedos may also  
451 contain a greater diversity of microbial products such as enzymes.

452 We have sought to address this possibility by screening for esterases and lipases from the  $\alpha/\beta$ -  
453 hydrolase fold superfamily in microbial communities inhabiting the Los Ruedos AMD site. These  
454 enzymes are desired tools for biocatalysis in a variety of industrial sectors (Ferrer et al., 2015; Daiha  
455 et al., 2015). Microorganisms that can survive under low pH values similar to those in Los Ruedos  
456 (pH ~2) could be good sources of enzymes that can be used, for example, as additives in detergents,  
457 for the biobleaching of pulp and paper, in the clean-up of effluent streams from the textile processing  
458 industry, and in the degradation of plastics (Gomes et al., 2003; Adrio and Demain, 2014; Nchedo  
459 Ariole and George-West, 2020) and other polymers (Fütturer et al., 2004).

460 We used two complementary approaches for enzyme mining. A sequence-based metagenomic  
461 approach that searched for homologous enzymes in the metagenomic sequence data and function-  
462 driven screens in which expression libraries were used to identify, by using specific colorimetric  
463 substrates (Ferrer et al., 2016; Peña-García et al., 2016), clones containing enzymes of interest that  
464 could be missed in shallow metagenomics sequencing. By using both approaches, we identified 16  
465 sequences potentially encoding esterases and lipases. The amino acid sequences were distantly  
466 related to sequences found in other AMD formations, which was in agreement with the distinct Los  
467 Ruedos-specific populations (Méndez-García et al., 2014). Indeed, we only observed some degree of  
468 sequence identity (27-54%) to 3 homologs from the Carnoulès (lead-zinc) mine, France (Bertin et al.,  
469 2011) in 6 of 16 sequences. In addition, the large differences among the recovered enzymes may  
470 correspond to the high population diversity that characterizes the Los Ruedos site (Méndez-García et  
471 al., 2014).

472 Notably, activity-based screens did not yield any active clones from the library created from the  
473 anoxic lowermost strata (B1B), while they yielded 10 active clones from the library created from the  
474 oxic uppermost strata (B1A). Thus, we searched for such enzymes in B1B by screening sequence  
475 data generated in a previous study (Méndez-García et al., 2014). It is plausible that the presence of  
476 low-O<sub>2</sub>-adapted microbial species in B1B, in contrast to the aerobic species in B1A, may account for

477 the low efficiency of heterologous gene expression after cloning of the genetic material in the *E. coli*  
478 host and, possibly, the lower efficiency of the screening tests in the B1B library compared to that  
479 obtained for B1A. However, the fact that similar proportions of identified proteins (by naïve and  
480 sequence screening) in B1A (7 of 12) and B1B (2 of 4) could be produced as soluble active proteins  
481 when expressed in *E. coli* suggests that this may not be the only reason explaining the absence of  
482 positive clones in the B1B library. We cannot rule out that the native promoters of the partial genes  
483 from microorganisms inhabiting B1B cloned in the pCCFOS1 fosmids were inactive in *E. coli*,  
484 resulting in failed active clones on the plates. The data provided in **Tables 2** and **3** revealed that B1B  
485 enzymes were among the least-active enzymes among all hydrolases identified and characterized in  
486 the present study, and it is therefore also plausible that the low efficiency of the screening tests may  
487 have been due to the low activity level of enzymes from microorganisms inhabiting the anoxic B1B  
488 compartment. Additionally, it is plausible that different screening conditions (temperature, pH,  
489 inductor concentration, etc.) may be needed to detect other active proteins and that the enzymes from  
490 B1B would be more active under other assay conditions, the investigation of which is beyond the  
491 scope of the present study.

492       Regardless of the problems associated with the screening efficiency in different environments,  
493 including extreme AMD formations such as Los Ruedos, the analysis of the optimal pH profile of 10  
494 out of the 16 hydrolases that could be produced in active form additionally revealed that their optimal  
495 pH was in the range from 7.0 to 9.0. This finding suggests that all hydrolases are presumptively  
496 produced intracellularly by acidophiles that thrive in the acidic Los Ruedos environment with a pH  
497 of 2.0. A similar phenotype has been found for other enzymes from AMD inhabitants, such as ATP-  
498 dependent DNA ligase from "*Ferroplasma acidarmanus*" Fer1 (Jackson et al., 2007) and ene-  
499 reductase from "*Ferrovum*" sp. JA12 (Scholtissek et al., 2016), with pH optima of 6.0-7.0. However,  
500 we observed that most of the enzymes showed a slightly acid-stable phenotype, retaining ~33-68% of  
501 activity at pH 5.5. It is plausible that the identification of enzymes with neutral-like pH optima is a  
502 consequence of screening tests performed at neutral pH, using a vector and host that allow mostly  
503 intracellular proteins to be produced and that presumably acid-stable enzymes could not be detected.  
504 In the future, performing naïve screens at such low pH values may help obtain additional active  
505 clones. However, while specific adaptations need to be explored in great detail, the retention of a  
506 high activity level at a slightly acidic pH might be attributed to the prevalence of acidic amino acids  
507 (negatively charged at a neutral pH) on the surfaces of these enzymes (**Supplementary Figure 2**), as  
508 reported for other proteins from acidophiles (Wu et al., 2020). Indeed, the relative frequencies of  
509 acidic residues in proteins in this study ranged from 67 to 54%, except for Est<sub>A8</sub> (37%). As no major  
510 differences in pH profiles were observed when comparing the enzymes with the highest (Est<sub>A1</sub>: 67%)  
511 and lowest (Est<sub>A8</sub>: 37%) percentages of acidic residues, it is possible that other factors affect the  
512 activity and stability of the studied proteins from the Los Ruedos site. An example of this is the  
513 differences in stability against pH and temperature of Est<sub>A5</sub> and Est<sub>A6</sub>, which show very different  
514 features and have only a two amino acid difference, despite having the same percentage of acidic  
515 residues.

516       Furthermore, the biochemical properties of the esterases reported in this study revealed that all  
517 enzymes showed an activity–stability trade-off characteristic of mesophilic-adapted enzymes (from  
518 30 to 65 °C), which is a phenotype that has also been found for enzymes from other AMD inhabitants  
519 (Scholtissek et al., 2016; Golyshina et al., 2006; Jackson et al., 2007; Ohara et al., 2014). It is  
520 noticeable, however, that 5 of 10 characterized enzymes retained at least 50% of their maximal  
521 activity at temperatures as low as 12 °C. The fact that the Los Ruedos site is characterized by a  
522 relatively low temperature compared to other AMD sites (Méndez-García et al., 2014) may account

523 for this low-temperature-active phenotype. However, the lack of biochemical information on  
524 enzymes from other AMD sites does not allow us to validate this assumption.

525 Finally, it should be emphasized that the activity levels of the characterized enzymes (maximum  
526 for the best *p*NP substrates: approx. 680 to 3 units/mg, depending on the hydrolase) were in the range  
527 of other reported enzymes of different origins with esterase and lipase activities (Ferrer et al., 2015;  
528 Martínez-Martínez et al., 2018). The data suggest that the low-O<sub>2</sub>-adapted microbial species  
529 developed in the anoxic lowermost (B1B) sediment-attached strata do contain less-active enzymes  
530 than those developed in the oxic uppermost (B1A) strata under the conditions used herein. Whether  
531 this is typical *in vivo* or is a result of bias due to the assay conditions would require the  
532 characterization of a larger number of enzymes from both microenvironments in the Los Ruedos  
533 AMD system. The capacity of six of the enzymes from the Los Ruedos AMD formation, and thus  
534 the bacteria that contain them, for degrading acrylic- and terephthalate-like esters is noticeable. These  
535 enzymes could potentially be of use in developing plastic degradation strategies that have yet to be  
536 explored. In this context, the taxonomic distribution of top protein hits, as well as the results of  
537 genome linguistics analysis, suggested that the metagenomic fragments containing the six  
538 characterized enzymes that can potentially degrade plastic substrates most likely belong to  
539 *Actinobacteria* (genera related to *Acidithrix* and *Acidimicrobium/Ferrimicrobium*), *Acidobacteria*  
540 and *Proteobacteria* (some are related to *Acidiphilium*). These are groups of acidophiles that have  
541 been largely neglected with respect to enzyme discovery.

542 PET-degrading bioprospecting has shown that only a tiny fraction of carboxylic ester hydrolases  
543 can degrade PET and its intermediates BHET and MHET, including Actinomycetes (i.e.,  
544 *Thermobifida*, *Thermomonospora*, and *Saccharomonospora*), *Bacillus*, *Firmicutes* (e.g.,  
545 *Clostridium*), *Bacteroidetes*, *Proteobacteria* (e.g., *Pseudomonas*, *Enterobacteria*, and *Ideonella*  
546 *sakaiensis*), and fungi (*Fusarium* and *Thermomyces (Humicola)*) (for a recent example, see Yoshida  
547 et al., 2016; Danso et al., 2018; Bollinger et al., 2020; Yan et al., 2021). In this study, we found that  
548 bacteria from the genera *Acidithrix* (the host of Est<sub>A1</sub>), *Acidimicrobium/Ferrimicrobium* (the host of  
549 Est<sub>A2</sub>) and unknown genera from the phylum *Proteobacteria* (the hosts of Est<sub>A5</sub>, Est<sub>A6</sub>, Est<sub>A8</sub>, and  
550 Est<sub>B2</sub>) could degrade BHET and could potentially degrade PET or PET oligomers under conditions  
551 yet to be explored, as no PET hydrolysis was detected under the assay conditions employed herein.  
552 Thus, the metagenomics approach applied herein expands the range of microorganisms containing  
553 enzymes supporting BHET hydrolysis and, possibly, PET depolymerization. For effective PET  
554 hydrolysis, in addition to a high degradation rate at 40-70°C, a broad range of pH stability (toward  
555 both the alkaline and acidic ranges) is one of the prerequisites of applied enzymes (Maurya et al.,  
556 2020), and these features were characteristic of some of the esterases from Los Ruedos reported  
557 herein. Further studies will reveal the catalytic efficiency and stability of hydrolases from Los  
558 Ruedos AMD systems to establish PET degradation systems or to support these systems in  
559 combination with other known PET-degrading enzymes.

560 It is plausible that the capacity to degrade plastic substrates comes from the adaptation of the  
561 active sites of enzymes to metabolize microbial polymeric substances that are naturally occurring in  
562 AMDs. Thus, in Los Ruedos, as in other AMDs such as the Richmond Mine at Iron Mountain  
563 (Martínez-Martínez et al., 2013; Jiao et al., 2010; Jiao et al., 2011), the organisms present might  
564 contribute to the use/degradation of extracellular polymeric substances (EPS), which requires a broad  
565 range of enzymes (Flemming and Wingender, 2010).

## 566 5 Data Availability Statement

567 The original contributions presented in the study are included in the article/**Supplementary**  
568 **Material**, and further inquiries can be directed to the corresponding author/s.

## 569 **6 Conflict of Interest**

570 The authors declare that the research was conducted in the absence of any commercial or financial  
571 relationships that could be construed as a potential conflict of interest.

## 572 **7 Author Contributions**

573 MF and AIP conceived this study. MMM contributed to gene cloning and expression. PV, MMM, LF-  
574 L, and MF performed biochemical data and interpreted the data. SR, VG performed 3D modelling.  
575 CMG, and MF contributed sample processing and library construction. OVG contributed phylogenetic  
576 analysis. MF drafted and revised the manuscript. All authors discussed, read, approved the manuscript,  
577 and authorized its submission for publication.

## 578 **8 Funding**

579 This study was conducted under the auspices of the FuturEnzyme Project funded by the European  
580 Union's Horizon 2020 Research and Innovation Programme under Grant Agreement No. 101000327.  
581 We also acknowledge financial support under Grants PCIN-2017-078 (within the Marine  
582 Biotechnology ERA-NET, GA No. 604814) (M.F.), BIO2017-85522-R (M.F.), PID2020-112758RB-  
583 I00 (M.F.), PID2019-106370RB-I00 (V.G.) and PDC2021-121534-I00 (M.F.) from the Ministerio de  
584 Economía, Industria y Competitividad, Ministerio de Ciencia e Innovación, Agencia Estatal de  
585 Investigación (AEI) (Digital Object Identifier 10.13039/501100011033), Fondo Europeo de  
586 Desarrollo Regional (FEDER) and the European Union ("NextGenerationEU/PRTR"), and Grant  
587 2020AEP061 (M.F.) from the Agencia Estatal CSIC. O.V.G acknowledges the support of the Centre  
588 for Environmental Biotechnology Project funded by the European Regional Development Fund  
589 (ERDF) via the Welsh Government. S. R. thanks the Spanish Ministry of Science and Innovation for  
590 a PhD fellowship (FPU19/00608).

## 591 **9 Acknowledgments**

592 The authors acknowledge David Almendral for supporting the circular dichroism analysis and Rafael  
593 Bargiela for preparation of Figure 2. The authors acknowledge the support of Cristina Coscolín for  
594 supporting the BHET degradation tests and Jesús Sánchez for the support in the study of AMD  
595 systems and the evaluation and review of this work.

## 596 **10 References**

- 597 Adrio, J.L., Demain, A.L. (2014). Microbial enzymes: tools for biotechnological processes.  
598 *Biomolecules*. 4, 117-139.
- 599 Alcaide, M., Tchigvintsev, A., Martinez-Martinez, M., Popovic, A., Reva, O.N., Lafraya, A.,  
600 Bargiela, R., Nechitaylo, T.Y., Matesanz, R., Cambon-Bonavita, M.A., Jebbar, M., Yakimov,  
601 M.M., Savchenko, A., Golyshina, O.V., Yakunin, A.F., Golyshin, P.N., Ferrer, M. (2015).  
602 Identification and characterization of carboxyl esterases of gill chamber-associated microbiota in  
603 the deep-sea shrimp *Rimicaris exoculata* by using functional metagenomics. *Appl Environ*  
604 *Microbiol.* 81, 2125-2136.

- 605 Altschul, S.F., Madden, T.L., Schäffer, A.A., Zhang, J., Zhang, Z., Miller, W., Lipman, D.J. (1997).  
606 Gapped BLAST and PSI-BLAST: a new generation of protein database search programs.  
607 *Nucleic Acids Res.* 25, 3389-3402.
- 608 Arpigny, J.L., Jaeger, K.E. (1999). Bacterial lipolytic enzymes: classification and properties.  
609 *Biochem J* 343:177-183.
- 610 Baker, B.J., Comolli, L.R., Dick, G.J., Hauser, L.J., Hyatt, D., Dill, B.D., Land, M.L., Verberkmoes,  
611 N.C., Hettich, R.L., Banfield, J.F. (2010). Enigmatic, ultrasmall, uncultivated Archaea. *Proc*  
612 *Natl Acad Sci U S A* 107, 8806-8811.
- 613 Baker, B.J., Tyson, G.W., Webb, R.I., Flanagan, J., Hugenholtz, P., Allen, E.E., Banfield, J.F.  
614 (2006). Lineages of acidophilic archaea revealed by community genomic analysis. *Science* 314,  
615 1933-1935.
- 616 Barth, S., Fischer, M., Schmid, R.D., Pleiss, J. (2004). The database of epoxide hydrolases and  
617 haloalkane dehalogenases: one structure, many functions. *Bioinformatics.* 20, 2845-2847.
- 618 Baweja, M., Nain, L., Kawarabayasi, Y. & Shukla, P. (2016) Current technological improvements in  
619 enzymes toward their biotechnological applications. *Frontiers in Microbiology*, 7, 1–13.
- 620 Bertin, P.N., Heinrich-Salmeron, A., Pelletier, E., Goulhen-Chollet, F., Arsène-Ploetze, F., Gallien,  
621 S., Lauga, B., Casiot, C., Calteau, A., Vallenet, D., Bonnefoy, V., Bruneel, O., Chane-Woon-  
622 Ming, B., Cleiss-Arnold, J., Duran, R., Elbaz-Poulichet, F., Fonknechten, N., Giloteaux, L.,  
623 Halter, D., Koechler, S., Marchal, M., Mornico, D., Schaeffer, C., Smith, A.A., Van Dorselaer,  
624 A., Weissenbach, J., Médigue, C., Le Paslier, D. (2011). Metabolic diversity among main  
625 microorganisms inside an arsenic-rich ecosystem revealed by meta- and proteo-genomics. *ISME*  
626 *J.* 5, 1735-1747.
- 627 Bhattacharyya, S., Banerjee, P.C., Das, P.K. (1990). A plasma-membrane associated ATPase from  
628 the acidophilic bacterium *Acidiphilium cryptum*. *Biochem Cell Biol.* 68, 1222-1225.
- 629 Bollinger, A., Thies, S., Knieps-Grünhagen, E., Gertzen, C., Kobus, S., Höppner, A., Ferrer, M.,  
630 Gohlke, H., Smits, S.H.J., Jaeger, K.E. (2020). A Novel polyester hydrolase from the marine  
631 bacterium *Pseudomonas aestusnigri* - Structural and functional insights. *Front Microbiol.* 11,  
632 114.
- 633 Bradford, M.M. (1976). A rapid and sensitive method for the quantification of microgram quantities  
634 of protein utilizing the principle of protein-dye binding. *Anal Biochem.* 72, 248-254.
- 635 Brugna, M., Nitschke, W., Asso, M., Guigliarelli, B., Lemesle-Meunier, D., Schmidt, C. (1999).  
636 Redox components of cytochrome bc-type enzymes in acidophilic prokaryotes. II. The Rieske  
637 protein of phylogenetically distant acidophilic organisms. *J Biol Chem.* 274, 16766-16772.
- 638 Cai, K., Delaviz, Y., Banh, M., Guo, Y., Santerre, J.P. (2014). Biodegradation of composite resin  
639 with ester linkages: identifying human salivary enzyme activity with a potential role in the  
640 esterolytic process. *Dent Mater.* 30(8), 848-60.



- 641 Chen, L.X., Huang, L.N., Méndez-García, C., Kuang, J.L., Hua, Z.S., Liu, J., Shu, W.S. (2016).  
642 Microbial communities, processes and functions in acid mine drainage ecosystems. *Curr Opin*  
643 *Biotechnol.* 38, 150-158.
- 644 Chen, L.X., Méndez-García, C., Dombrowski, N., Servín-Garcidueñas, L.E., Eloë-Fadrosh, E.A.,  
645 Fang, B.Z., Luo, Z.H., Tan, S., Zhi, X.Y., Hua, Z.S., Martínez-Romero, E., Woyke, T., Huang,  
646 L.N., Sánchez, J., Peláez, A.I., Ferrer, M., Baker, B.J., Shu, W.S. (2018). Metabolic versatility of  
647 small archaea Micrarchaeota and Parvarchaeota. *ISME J* 12, 756–775.
- 648 Cherney, M.M., Zhang, Y., Solomonson, M., Weiner, J.H., James, M.N. (2010). Crystal structure of  
649 sulfide:quinone oxidoreductase from *Acidithiobacillus ferrooxidans*: insights into sulfidotrophic  
650 respiration and detoxification. *J Mol Biol.* 398, 292-305.
- 651 Daiha Kde, G., Angeli, R., de Oliveira, S.D., Almeida, R.V. (2015). Are lipases still important  
652 biocatalysts? a study of scientific publications and patents for technological forecasting. *PLoS*  
653 *One.* 10, e0131624.
- 654 Danso, D., Schmeisser, C., Chow, J., Zimmermann, W., Wei, R., Leggewie, C., Li, X., Hazen, T.,  
655 Streit, W.R. (2018). New insights into the function and global distribution of polyethylene  
656 terephthalate (PET)-degrading bacteria and enzymes in marine and terrestrial metagenomes.  
657 *Appl Environ Microbiol.* 84, e02773-17.
- 658 Delavat, F., Phalip, V., Forster, A., Plewniak, F., Lett, M.C., Lièvremon, D. (2012). Amylases  
659 without known homologues discovered in an acid mine drainage: significance and impact. *Sci*  
660 *Rep.* 2, 354.
- 661 Donahue, Craig J., Exline, Jennifer A., Warner Cynthia. (2003). Chemical recycling of pop bottles:  
662 The synthesis of dibenzyl terephthalate from the plastic polyethylene terephthalate. *J. Chem.*  
663 *Educ.* 80, 1, 79.
- 664 Dopson, M., Baker-Austin, C., Hind, A., Bowman, J.P., Bond, P.L. (2004). Characterization of  
665 *Ferroplasma* isolates and *Ferroplasma acidarmanus* sp. nov., extreme acidophiles from acid  
666 mine drainage and industrial bioleaching environments. *Appl Environ Microbiol.* 70, 2079-2088.
- 667 Egorova, M.A., Tsaplina, I.A., Zakharchuk, L.M., Bogdanova, T.I., Krasil'nikova, E.N. (2004).  
668 Effect of cultivation conditions on the growth and activities of sulfur metabolism enzymes and  
669 carboxylases of *Sulfobacillus thermosulfidooxidans* subsp. asporogenes strain 41. *Prikl Biokhim*  
670 *Mikrobiol.* 40, 448-454.
- 671 Ferrer, M., Bargiela, R., Martínez-Martínez, M., Mir, J., Koch, R., Golyshina, O.V., Golyshin, P.N.  
672 (2015). Biodiversity for biocatalysis: A review of the  $\alpha/\beta$ -hydrolase fold superfamily of  
673 esterases-lipases discovered in metagenomes. *Biocatal Biotransform.* 33, 235-249.
- 674 Ferrer, M., Martínez-Martínez, M., Bargiela, R., Streit, W.R., Golyshina, O.V., Golyshin, P.N.  
675 (2016). Estimating the success of enzyme bioprospecting through metagenomics: current status  
676 and future trends. *Microb Biotechnol.* 9, 22-34.
- 677 Ferrer, M., Méndez-García, C., Bargiela, R., Chow, J., Alonso, S., García-Moyano, A., Bjerga, G.,  
678 Steen, I., Schwabe, T., Blom, C., Vester, J., Weckbecker, A., Shahgaldian, P., de Carvalho, C.,  
679 Meskys, R., Zanaroli, G., Glöckner, F., Fernández-Guerra, A., Thambisetty, S., de la Calle, F.,

- 680 Golyshina, O., Yakimov, M., Jaeger, K.E., Yakunin, A., Streit, W.R., McMeel, O., Calewaert,  
681 J.B., Tonné, N., Golyshin, P.N. (2019). Decoding the ocean's microbiological secrets for marine  
682 enzyme biodiscovery. *FEMS Microbiol. Lett.* 366, 0378-1097.
- 683 Finer, Y., Santerre, J.P. (2004). Salivary esterase activity and its association with the biodegradation  
684 of dental composites. *J Dent Res.* 83(1), 22-26.
- 685 Fischer, M., Pleiss, J. (2003). The Lipase Engineering Database: a navigation and analysis tool for  
686 protein families. *Nucleic Acids Res.* 31, 319-321.
- 687 Flemming, HC., Wingender, J. (2010). The biofilm matrix. *Nat Rev Microbiol* 8, 623-633.
- 688 Fütterer, O., Angelov, A., Liesegang, H., Gottschalk, G., Schleper, C., Schepers, B., Dock, C.,  
689 Antranikian, G., Liebl, W. (2004). Genome sequence of *Picrophilus torridus* and its implications  
690 for life around pH 0. *Proc Natl Acad Sci USA.* 101, 9091-9096.
- 691 Gavrilov, S.N., Korzhenkov, A.A., Kublanov, I.V., Bargiela, R., Zamana, L.V., Popova, A.A.,  
692 Toshchakov, S.V., Golyshin, P.N., Golyshina, O.V. (2019). Microbial communities of  
693 polymetallic deposits' acidic ecosystems of continental climatic zone with high temperature  
694 contrasts. *Front Microbiol.* 10, 1573.
- 695 Giunta, C.I., Cea-Rama, I., Alonso, S., Briand, M.L., Bargiela, R., Coscolín, C., Corvini, P.F., Ferrer,  
696 M., Sanz-Aparicio, J., Shahgaldian, P. (2020) Tuning the properties of natural promiscuous  
697 enzymes by engineering their nano-environment. *ACS Nano* 14, 17652-17664.
- 698 Golyshina, O.V. (2011). Environmental, biogeographic, and biochemical patterns of archaea of the  
699 family *Ferroplasmaceae*. *Appl Environ Microbiol.* 77, 5071-5078.
- 700 Golyshina, O.V., Golyshin, P.N., Timmis, K.N., Ferrer, M. (2006). The 'pH optimum anomaly' of  
701 intracellular enzymes of *Ferroplasma acidiphilum*. *Environ Microbiol.* 8, 416-425.
- 702 Golyshina, O.V., Lünsdorf, H., Kublanov, I.V., Goldenstein, N.I., Hinrichs, K.U., Golyshin, P.N.  
703 (2016). The novel extremely acidophilic, cell-wall-deficient archaeon *Cuniculiplasma*  
704 *divulgatum* gen. Nov., sp. nov. represents a new family, *Cuniculiplasmataceae* fam. nov., of the  
705 order Thermoplasmatales. *Int J Syst Evol Microbiol.* 66, 332-340.
- 706 Golyshina, O.V., Pivovarova, T.A., Karavaiko, G.I., Kondratéva, T.F., Moore, E.R., Abraham, W.R.,  
707 Lünsdorf, H., Timmis, K.N., Yakimov, M.M., Golyshin, P.N. (2000). *Ferroplasma acidiphilum*  
708 gen. nov., sp. nov., an acidophilic, autotrophic, ferrous-iron-oxidizing, cell-wall-lacking,  
709 mesophilic member of the *Ferroplasmaceae* fam. nov., comprising a distinct lineage of the  
710 Archaea. *Int J Syst Evol Microbiol.* 3, 997-1006.
- 711 Golyshina, O.V., Yakimov, M.M., Lünsdorf, H., Ferrer, M., Nimtz, M., Timmis, K.N., Wray, V.,  
712 Tindall, B.J., Golyshin, P.N. (2009). *Acidiplasma aeolicum* gen. nov., sp. nov., a euryarchaeon  
713 of the family Ferroplasmaceae isolated from a hydrothermal pool, and transfer of *Ferroplasma*  
714 *cupricumulans* to *Acidiplasma cupricumulans* comb. nov. *Int J Syst Evol Microbiol.* 59, 2815-  
715 2823.

- 716 Gomes, I., Gomes, J., Steiner, W. (2003). Highly thermostable amylase and pullulanase of the  
717 extreme thermophilic eubacterium *Rhodothermus marinus*: production and partial  
718 characterization. *Bioresour Technol.* 90, 207-214.
- 719 Guazzaroni, M.E., Morgante, V., Mirete, S., González-Pastor, J.E. (2013). Novel acid resistance  
720 genes from the metagenome of the Tinto River, an extremely acidic environment. *Environ*  
721 *Microbiol.* 15, 1088-1102.
- 722 Hajighasemi, M., Tchigvintsev, A., Nocek, B., Flick, R., Popovic, A., Hai, T., Khusnutdinova, A.N.,  
723 Brown, G., Xu, X., Cui, H., Anstett, J., Chernikova, T.N., Bröls, T., Le Paslier, D., Yakimov,  
724 M.M., Joachimiak, A., Golyshina, O.V., Savchenko, A., Golyshin, P.N., Edwards, E.A.,  
725 Yakunin, A.F. (2018). Screening and characterization of novel polyesterases from environmental  
726 metagenomes with high hydrolytic activity against synthetic polyesters. *Environ Sci Technol.* 52,  
727 12388-12401.
- 728 He, Y., Zhang, F., Saleh, E., Vaithilingam, J., Aboulkhair, N., Begines, B., Tuck, C.J., Hague,  
729 R.J.M., Ashcroft, I.A., Wildman, R.D. (2017). A tripropylene glycol diacrylate-based polymeric  
730 support ink for material jetting. *Additive Manufacturing.* 16, 2017, 153-161.
- 731 Huang, Y., Krauss, G., Cottaz, S., Driguez, H., Lipps, G. (2005). A highly acid-stable and  
732 thermostable endo-beta-glucanase from the thermoacidophilic archaeon *Sulfolobus solfataricus*.  
733 *Biochem J.* 385, 581-588.
- 734 Huang, L-N., Kuang, J-L., Shu, W-S. (2016). Microbial ecology and evolution in the acid mine  
735 drainage model system. *Trends Microbiol.* 24, 581-593.
- 736 Hügler, M., Krieger, R.S., Jahn, M., Fuchs, G. (2003). Characterization of acetyl-CoA/propionyl-  
737 CoA carboxylase in *Metallosphaera sedula*. Carboxylating enzyme in the 3-hydroxypropionate  
738 cycle for autotrophic carbon fixation. *Eur J Biochem.* 270, 736-744.
- 739 Inagaki, K., Tomono, J., Kishimoto, N., Tano, T., Tanaka, H. (1993). Transformation of the  
740 acidophilic heterotroph *Acidiphilium facilis* by electroporation. *Biosci Biotechnol Biochem.* 57,  
741 1770-1771.
- 742 Jackson, B.R., Noble, C., Lavesa-Curto, M., Bond, P.L., Bowater, R.P. (2007). Characterization of an  
743 ATP-dependent DNA ligase from the acidophilic archaeon "*Ferroplasma acidarmanus*" Fer1.  
744 *Extremophiles.* 11, 315-327.
- 745 Jiao, Y., Cody, G.D., Harding, A.K., Wilmes, P., Schrenk, M., Wheeler, K.E., Banfield, J.F., Thelen,  
746 M.P. (2010). Characterization of extracellular polymeric substances from acidophilic microbial  
747 biofilms. *Appl Environ Microbiol.* 76, 2916-2922.
- 748 Jiao, Y., D'haeseleer, P., Dill, B.D., Shah, M., Verberkmoes, N.C., Hettich, R.L., Banfield, J.F.,  
749 Thelen, M.P. (2011). Identification of biofilm matrix associated proteins from an acid mine  
750 drainage microbial community. *Appl Environ Microbiol.* 77, 5230-5237.
- 751 Johnson, D.B., Quatrini, R. (2020). Acidophile microbiology in space and time. *Curr Issues Mol*  
752 *Biol.* 39, 63-76.

- 753 Jumper, J., Evans, R., Pritzel, A., Green, T., Figurnov, M., Ronneberger, O., Tunyasuvunakool, K.,  
754 Bates, R., Žídek, A., Potapenko, A., Bridgland, A., Meyer, C., Kohl, S., Ballard, A., Cowie, A.,  
755 Romera-Paredes, B., Nikolov, S., Jain, R., Adler, J., Back, T., Petersen, S., Reiman, D., Clancy,  
756 E., Zielinski, M., Steinegger, M., Pacholska, M., Berghammer, T., Bodenstein, S., Silver, D.,  
757 Vinyals, O., Senior, A., Kavukcuoglu, K., Kohli, P., Hassabis, D. (2021). Highly accurate  
758 protein structure prediction with AlphaFold. *Nature*. 596, 583–589.
- 759 Kanao, T., Matsumoto, C., Shiraga, K., Yoshida, K., Takada, J., Kamimura, K. (2010). Recombinant  
760 tetrathionate hydrolase from *Acidithiobacillus ferrooxidans* requires exposure to acidic  
761 conditions for proper folding. *FEMS Microbiol Lett*. 309, 43-47.
- 762 Kanao, T., Nakayama, H., Kato, M., Kamimura, K. (2014). The sole cysteine residue (Cys301) of  
763 tetrathionate hydrolase from *Acidithiobacillus ferrooxidans* does not play a role in enzyme  
764 activity. *Biosci Biotechnol Biochem*. 78, 2030-2035.
- 765 Kikumoto, M., Nogami, S., Kanao, T., Takada, J., Kamimura, K. (2013). Tetrathionate-forming  
766 thiosulfate dehydrogenase from the acidophilic, chemolithoautotrophic bacterium  
767 *Acidithiobacillus ferrooxidans*. *Appl Environ Microbiol*. 79, 113-120.
- 768 Koivula, T.T., Hemilä, H., Pakkanen, R., Sibakov, M., Palva, I. (1993). Cloning and sequencing of a  
769 gene encoding acidophilic amylase from *Bacillus acidocaldarius*. *J Gen Microbiol*. 139, 2399-  
770 2407.
- 771 Korzhenkov, A.A., Toshchakov, S.V., Bargiela, R., Gibbard, H., Ferrer, M., Teplyuk, A.V., Jones,  
772 D.L., Kublanov, I.V., Golyshin, P.N., Golyshina, O.V. (2019). Archaea dominate the microbial  
773 community in an ecosystem with low-to-moderate temperature and extreme acidity. *Microbiome*  
774 7, 11.
- 775 Laemmli, U.K. (1970). Cleavage of structural proteins during the assembly of the head of  
776 bacteriophage T4. *Nature*. 227, 680-685.
- 777 López, G., Chow, J., Bongen, P., Lauinger, B., Pietruszka, J., Streit, W.R., Baena, S. (2014). A novel  
778 thermoalkalostable esterase from *Acidicaldus* sp. strain USBA-GBX-499 with enantioselectivity  
779 isolated from an acidic hot springs of Colombian Andes. *Appl Microbiol Biotechnol*. 98, 8603-  
780 8616.
- 781 Martínez-Martínez, M., Alcaide, M., Tchigvintsev, A., Reva, O., Polaina, J., Bargiela, R.,  
782 Guazzaroni, M.E., Chicote, Á., Canet, A., Valero, F., Rico Eguizabal, E., Guerrero Mdel, C.,  
783 Yakunin, A.F., Ferrer, M. (2013). Biochemical diversity of carboxyl esterases and lipases from  
784 Lake Arreo (Spain): a metagenomic approach. *Appl Environ Microbiol*. 79, 3553-3562.
- 785 Martínez-Martínez, M., Coscolín, C., Santiago, G., Chow, J., Stogios, P.J., Bargiela, R., Gertler, C.,  
786 Navarro-Fernández, J., Bollinger, A., Thies, S., Méndez-García, C., Popovic, A., Brown, G.,  
787 Chernikova, T.N., García-Moyano, A., Bjerga, G.E.K., Pérez-García, P., Hai, T., Del Pozo,  
788 M.V., Stokke, R., Steen, I.H., Cui, H., Xu, X., Nocek, B.P., Alcaide, M., Distaso, M., Mesa, V.,  
789 Peláez, A.I., Sánchez, J., Buchholz, P.C.F., Pleiss, J., Fernández-Guerra, A., Glöckner, F.O.,  
790 Golyshina, O.V., Yakimov, M.M., Savchenko, A., Jaeger, K.E., Yakunin, A.F., Streit, W.R.,  
791 Golyshin, P.N., Guallar, V., Ferrer, M., The Inmare Consortium. (2018). Determinants and  
792 prediction of esterase substrate promiscuity patterns. *ACS Chem Biol*. 13, 225-234.

- 793 Maurya, A., Bhattacharya, A., Khare, S.K. (2020). Enzymatic remediation of polyethylene  
794 terephthalate (PET)-based polymers for effective management of plastic wastes: An Overview.  
795 *Front Bioeng Biotechnol.* 8, 602325.
- 796 Méndez-García, C., Mesa, V., Sprenger, R.R., Richter, M., Diez, M.S., Solano, J., Bargiela, R.,  
797 Golyshina, O.V., Manteca, Á., Ramos, J.L., Gallego, J.R., Llorente, I., Martins, dos Santos,  
798 V.A., Jensen, O.N., Peláez, A.I., Sánchez, J., Ferrer, M. (2014). Microbial stratification in low  
799 pH oxic and suboxic macroscopic growths along an acid mine drainage. *ISME J.* 8, 1259-1274.
- 800 Méndez-García, C., Peláez, A.I., Mesa, V., Sánchez, J., Golyshina, O.V., Ferrer, M. (2015).  
801 Microbial diversity and metabolic networks in acid mine drainage habitats. *Front Microbiol.* 6,  
802 475.
- 803 Ménigaud, S., Mallet, L., Picord, G., Churlaud, C., Borrel, A., Deschavanne, P. (2012). GOHTAM: a  
804 website for 'Genomic Origin of Horizontal Transfers, Alignment and Metagenomics'.  
805 *Bioinformatics.* 28, 1270-1271.
- 806 Meyer, B.H., Albers, S.V. (2014). AglB, catalyzing the oligosaccharyl transferase step of the  
807 archaeal N-glycosylation process, is essential in the thermoacidophilic crenarchaeon *Sulfolobus*  
808 *acidocaldarius*. *Microbiologyopen.* 3, 531-543.
- 809 Nchedo Ariole, C., George-West, O. (2020) Bioplastic degradation potential of microorganisms  
810 isolated from the soil. *Am J Chem Eng.* 4, 1.
- 811 Ohara, K., Unno, H., Oshima, Y., Hosoya, M., Fujino, N., Hirooka, K., Takahashi, S., Yamashita, S.,  
812 Kusunoki, M., Nakayama, T. (2014). Structural insights into the low pH adaptation of a unique  
813 carboxylesterase from *Ferroplasma*: altering the pH optima of two carboxylesterases. *J Biol*  
814 *Chem.* 289, 24499-24510.
- 815 Ohshima, T., Kawakami, R., Kanai, Y., Goda, S., Sakuraba, H. (2007). Gene expression and  
816 characterization of 2-keto-3-deoxygluconate kinase, a key enzyme in the modified Entner-  
817 Doudoroff pathway of the aerobic and acidophilic hyperthermophile *Sulfolobus tokodaii*. *Protein*  
818 *Expr Purif.* 54, 73-78.
- 819 Pellis, A., Cantone, S., Ebert, C., Gardossi, L. (2017). Evolving biocatalysis to meet bioeconomy  
820 challenges and opportunities. *New Biotechnol.* 40, 154-169.
- 821 Peña-García, C., Martínez-Martínez, M., Reyes-Duarte, D., Ferrer, M. (2016). High throughput  
822 screening of esterases, lipases and phospholipases in mutant and metagenomic libraries: a  
823 review. *Comb Chem High Throughput Screen.* 19, 605-615.
- 824 Placido, A., Hai, T., Ferrer, M., Chernikova, T.N., Distaso, M., Armstrong, D., Yakunin, A.F.,  
825 Toshchakov, S.V., Yakimov, M.M., Kublanov, I.V., Golyshina, O.V., Pesole, G., Ceci, L.R.,  
826 Golyshin, P.N. (2015). Diversity of hydrolases from hydrothermal vent sediments of the Levante  
827 Bay, Vulcano Island (Aeolian archipelago) identified by activity-based metagenomics and  
828 biochemical characterization of new esterases and an arabinopyranosidase. *Appl Microbiol*  
829 *Biotechnol.* 99, 10031-10046.
- 830 Pütz, A. (2006). Isolierung, identifizierung und biochemische charakterisierung dialkylphthalat  
831 spaltender esterases. PhD Thesis, HeinrichHeine-Universität, Düsseldorf, pp. 39-40.

- 832 Rao, L., Xue, Y., Zheng, Y., Lu, J.R., Ma, Y.A. (2013). A novel alkaliphilic bacillus esterase belongs  
833 to the 13(th) bacterial lipolytic enzyme family. *PloS One*. 8, e60645.
- 834 Reyes-Duarte, D., Ferrer, M., García-Arellano, H. (2012). Functional-based screening methods for  
835 lipases, esterases, and phospholipases in metagenomic libraries. *Methods Mol Biol*. 861, 101-  
836 113.
- 837 Santiago, G., Martínez-Martínez, M., Alonso, S., Bargiela, R., Coscolín, C., Golyshin, P.N., Guallar,  
838 V., Ferrer, M. (2018). Rational engineering of multiple active sites in an ester hydrolase.  
839 *Biochemistry* 57, 2245–2255
- 840 Scholtissek, A., Ullrich, S.R., Mühling, M., Schlömann, M., Paul, C.E., Tischler, D. (2016). A  
841 thermophilic-like ene-reductase originating from an acidophilic iron oxidizer. *Appl Microbiol*  
842 *Biotechnol*. 101, 2.
- 843 Sharma, A., Kawarabayasi, Y., Satyanarayana, T. (2012). Acidophilic bacteria and archaea: acid  
844 stable biocatalysts and their potential applications. *Extremophiles*. 16,1-19.
- 845 Sharmin, S., Yoshino, E., Kanao, T., Kamimura, K. (2016). Characterization of a novel thiosulfate  
846 dehydrogenase from a marine acidophilic sulfur-oxidizing bacterium, *Acidithiobacillus*  
847 *thiooxidans* strain SH. *Biosci Biotechnol Biochem*. 80, 273-278.
- 848 Smeulders, M.J., Pol, A., Venselaar, H., Barends, T.R., Hermans, J., Jetten, M.S., Op, den Camp,  
849 H.J. (2013). Bacterial CS<sub>2</sub> hydrolases from *Acidithiobacillus thiooxidans* strains are homologous  
850 to the archaeal catenane CS<sub>2</sub> hydrolase. *J Bacteriol*. 195, 4046-4056.
- 851 Thapa, S., Mishra, J., Arora, N., Mishra, P., Li, H., O'Hair, J., Bhatti, S., Zhou, S. (2020). Microbial  
852 cellulolytic enzymes: diversity and biotechnology with reference to lignocellulosic biomass  
853 degradation. *Rev Environ Sci Biotechnol*. 19, 621-648.
- 854 Van den Berg, B. (2010). Crystal structure of a full-length autotransporter. *J Mol Biol*. 396, 627-633.
- 855 Wakai, S., Ohmori, A., Kanao, T., Sugio, T., Kamimura, K. (2005). Purification and biochemical  
856 characterization of the F1-ATPase from *Acidithiobacillus ferrooxidans* NASF-1 and analysis of  
857 the atp operon. *Biosci Biotechnol Biochem*. 69, 1884-1891.
- 858 Wakai, S., Tsujita, M., Kikumoto, M., Manchur, M.A., Kanao, T., Kamimura, K. (2007). Purification  
859 and characterization of sulfide:quinone oxidoreductase from an acidophilic iron-oxidizing  
860 bacterium, *Acidithiobacillus ferrooxidans*. *Biosci Biotechnol Biochem*. 71, 2735-4272.
- 861 Wang, H., Liu, S., Liu, X., Li, X., Wen, Q., Lin, J. (2014). Identification and characterization of an  
862 ETHE1-like sulfur dioxygenase in extremely acidophilic *Acidithiobacillus* spp. *Appl Microbiol*  
863 *Biotechnol*. 98,7511-7522.
- 864 Wang, J., Yi, G., Ou, J., Liu, J., Liu, X. (2015). Cloning, expression, purification and characterization  
865 of two uracil-DNA glycosylases from *Sulfolobus acidocaldarius*. *Wei Sheng Wu Xue Ba*. 55,  
866 1036-1041.

- 867 Wu, X., Zhang, Q., Zhang, L., Liu, S., Chen, G., Zhang, H., Wang, L. (2020). Insights into the role of  
868 exposed surface charged residues in the alkali-tolerance of GH11 xylanase. *Front Microbiol.* 8,  
869 11, 872.
- 870 Yan, F., Wei, R., Cui, Q., Bornscheuer, U.T., Liu, Y.J. (2021). Thermophilic whole-cell degradation  
871 of polyethylene terephthalate using engineered *Clostridium thermocellum*. *Microb Biotechnol.*  
872 14, 374-385.
- 873 Yoshida, S., Hiraga, K., Takehana, T., Taniguchi, I., Yamaji, H., Maeda, Y., Toyohara, K.,  
874 Miyamoto, K., Kimura, Y., Oda, K. (2016). A bacterium that degrades and assimilates  
875 poly(ethylene terephthalate). *Science* 351, 1196-1199.
- 876 Yuan, T.Z., Yao, B., Luo, H.Y., Wang, Y.R., Wu, N.F., Fan, Y.L. (2005). Expression of acidophilic  
877 alpha-amylase from *Alicyclobacillus acidocaldarius*. *Sheng Wu Gong Cheng Xue Bao.* 21, 78-  
878 83.

**TABLE 1** | General sequence-based characteristics of Los Ruedos esterases.

Name	Acc. nr.	Contig bp (taxonomic origin [phylum, genus]) <sup>d</sup>	Identity and best hit <sup>e</sup>	pI	Putative catalytic triad <sup>f</sup>
EstA <sub>1</sub> <sup>a,b</sup>	KY010297	41280 ( <i>Actinomycetota, Acidithrix</i> )	99%; WP_052605564.1	4.62	Ser <sub>146</sub> , Asp <sub>193</sub> , His <sub>270</sub>
EstA <sub>2</sub> <sup>a,b</sup>	KY010298	33407 ( <i>Actinomycetota, Acidimicrobium/Ferrimicrobium</i> )	94%; NNN14078.1	5.03	Ser <sub>185</sub> , Asp <sub>316</sub> , His <sub>412</sub>
EstA <sub>3</sub> <sup>a,b</sup>	KY010300	32091 ( <i>Acidobacteria, a.a.</i> )	58%; WP_041839843	5.44	Ser <sub>83</sub> , Asp <sub>231</sub> , His <sub>234</sub>
EstA <sub>4</sub> <sup>a,b</sup>	KY010299	35459 ( <i>Proteobacteria, Acidiphilium</i> )	79%; OYV70855.1	5.53	Ser <sub>159</sub> , Asp <sub>254</sub> , His <sub>284</sub>
EstA <sub>5</sub> <sup>a,b</sup>	KY019260	26956 ( <i>Proteobacteria, a.a.</i> )	62%; ODU57651.1	5.43	Ser <sub>159</sub> , Asp <sub>254</sub> , His <sub>284</sub>
EstA <sub>6</sub> <sup>a,b</sup>	KY010302	39640 ( <i>Proteobacteria, a.a.</i> )	62%; ODU57651.1	5.32	Ser <sub>159</sub> , Asp <sub>254</sub> , His <sub>284</sub>
EstA <sub>7</sub> <sup>b,c</sup>	EQD63018.1	2621 ( <i>Proteobacteria, a.a.</i> )	64%; ODU34315	6.29	Ser <sub>123</sub> , Asp <sub>175</sub> , His <sub>207</sub>
EstA <sub>8</sub> <sup>a,b</sup>	KY010301	38626 ( <i>Proteobacteria, a.a.</i> )	56%; WP_063671588.1	10.04	Ser <sub>90</sub> , Asp <sub>237</sub> , His <sub>240</sub>
EstA <sub>9</sub> <sup>c</sup>	EQD66234.1	1763 ( <i>Proteobacteria, a.a.</i> )	53%; WP_055246968.1	7.12	Ser <sub>120</sub> , Asp <sub>188</sub> , His <sub>220</sub>
EstA <sub>10</sub> <sup>a</sup>	KY010303	16545 ( <i>Actinomycetota - Acidithrix</i> )	100%; WP_052605292.1	5.55	Ser <sub>75</sub> , Lys <sub>75</sub> , Tyr <sub>193</sub>
EstA <sub>11</sub> <sup>a</sup>	KY010304	40600 ( <i>Proteobacteria, a.a.</i> )	67%; WP_051488053	9.71	Asp <sub>506</sub> , His <sub>578</sub> , His <sub>582</sub>
EstA <sub>12</sub> <sup>a</sup>	KY010305	35290 ( <i>Bacteria, a.a.</i> )	41%; WP_009508720.1	9.65	Ser <sub>109</sub> , Asp <sub>315</sub> , His <sub>318</sub>
EstB <sub>1</sub> <sup>b,c</sup>	EQD71191.1	2283 ( <i>Proteobacteria, a.a.</i> )	69%; WP_049623914.1	5.89	Ser <sub>117</sub> , Asp <sub>165</sub> , His <sub>294</sub>
EstB <sub>2</sub> <sup>b,c</sup>	EQD52136.1	2483 ( <i>Proteobacteria, a.a.</i> )	48%; WP_055799051.1	6.11	Ser <sub>116</sub> , Asp <sub>164</sub> , His <sub>195</sub>
EstB <sub>3</sub> <sup>c</sup>	EQD26916.1	13465 ( <i>Proteobacteria, a.a.</i> )	49%; WP_026633329.1	5.7	Ser <sub>59</sub> , Asp <sub>313</sub> , His <sub>316</sub>
EstB <sub>4</sub> <sup>c</sup>	EQD55146.1	13877 ( <i>Actinobacteria, a.a.</i> )	39%; WP_051823767.1	6.07	Ser <sub>86</sub> , Asp <sup>?</sup> , His <sub>231</sub>

<sup>a</sup>Identified by naïve screen. <sup>b</sup>Protein expressed as active soluble form. <sup>c</sup>Identified by sequence-based screen from metagenomic sequencing data; accession number of the sequences in NCBI being ID PRJNA193663 (for B1A) and PRJNA193664 (for B1B). <sup>d</sup>As determined by GOHTAM database (Ménigaud et al., 2012) and TBLASTX; taxonomic assignment to phylum and genera are shown, with a.a. defining those for which ambiguous assignments below phylum level were obtained. <sup>e</sup>Best hit and identity as shown by TBLASTX. <sup>f</sup>Presumptive catalytic triad as found by 3 dimensional structure analysis and alignment with homologous proteins with solved crystal structures.

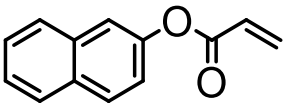
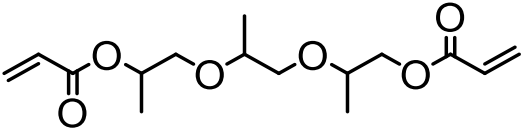
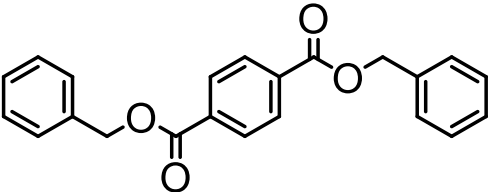
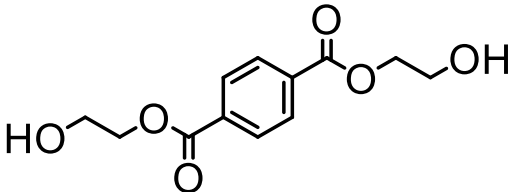


**TABLE 2** | Specific activity (U/mg pure protein) for each of the enzymes tested over a set of *p*NP esters of different lengths. Values calculated from triplicates at pH 8.0 and 30 °C.

Ester	Specific activity (U/mg protein)					
	<i>p</i> NPC <sub>2</sub>	<i>p</i> NPC <sub>3</sub>	<i>p</i> NPC <sub>4</sub>	<i>p</i> NPC <sub>8</sub>	<i>p</i> NPC <sub>10</sub>	<i>p</i> NPC <sub>12</sub>
EstA <sub>1</sub>	76.43±0.31	158.5±2.5	204.8±10.7	2.75±0.14	0.62±0.05	0.19±0.09
EstA <sub>2</sub>	30.39±0.19	50.56±0.78	27.68±0.83	1.60±0.01	0.82±0.08	0.16±0.05
EstA <sub>3</sub>	30.40±0.11	4.73±0.05	1.16±0.03	n.d. <sup>a</sup>	n.d. <sup>a</sup>	n.d. <sup>a</sup>
EstA <sub>4</sub>	28.39±2.8	280.4±8.7	196.1±2.7	32.55±2.67	11.19±0.48	0.100±0.03
EstA <sub>5</sub>	120.6±5.3	665.9±10.8	293.4±14.1	8.11±1.45	0.29±0.02	0.17±0.01
EstA <sub>6</sub>	520.1±1.7	679.8±9.8	467.7±6.4	11.93±0.06	0.37±0.02	0.12±0.01
EstA <sub>7</sub>	1.91±0.03	2.18±0.08	3.23±0.06	0.53±0.02	0.14±0.01	0.02±0.01
EstA <sub>8</sub>	14.07±0.95	26.13±0.71	70.39±0.16	24.81±0.09	0.95±0.06	0.85±0.02
EstB <sub>1</sub>	4.73±0.33	15.18±0.85	9.05±0.61	4.25±0.24	0.51±0.04	0.24±0.09
EstB <sub>2</sub>	2.32±0.01	3.06±0.03	2.17±0.05	0.54±0.04	0.12±0.02	0.04±0.01

<sup>a</sup>Not detected, activity level below detection limits under our assay conditions. Abbreviations as follows: *p*-nitrophenyl acetate (*p*NPC<sub>2</sub>), propionate (*p*NPC<sub>3</sub>) and butyrate (*p*NPC<sub>4</sub>), octanoate (*p*NPC<sub>8</sub>), decanoate (*p*NPC<sub>10</sub>) and decanoate (*p*NPC<sub>12</sub>).

**TABLE 3** | Specific activity (U/g pure protein) for each of the enzymes able to hydrolyze a set of structurally different plastic-related esters. Assays were performed in triplicate with values for each of the replicates given in the table with standard deviation. Values calculated at pH 8.0 and 30 °C.

Substrate	Structure	Specific activity (U/g pure protein)							
		EstA1	EstA2	EstA3	EstA4	EstA5	EstA6	EstA8	EstB2
2-Naphthyl acrylate		370.7 ± 20.3	37.7 ± 4.1	50.2 ± 0.4	1308 ± 79	n.d. <sup>1</sup>	n.d. <sup>1</sup>	748.1 ± 15.9	144.5 ± 10
Tri(propylene glycol) diacrylate		514.5 ± 36.3	4.9 ± 1.1	8.6 ± 0.7	3915 ± 48	n.d. <sup>1</sup>	n.d. <sup>1</sup>	1652 ± 75	73.5 ± 2.9
Dibenzyl terephthalate		n.d. <sup>a</sup>	n.d. <sup>a</sup>	n.d. <sup>a</sup>	n.d. <sup>1</sup>	n.d. <sup>1</sup>	n.d. <sup>1</sup>	432.2 ± 27.5	n.d. <sup>a</sup>
BHET <sup>b</sup>		308.3 ± 3.9	5.0 ± 1.0	n.d. <sup>a</sup>	n.d. <sup>a</sup>	26.7 ± 1.7	12.3 ± 0.4	336.9 ± 3.6	91.1 ± 3.2

<sup>a</sup>Not detected, activity level below detection limits under our assay conditions.

<sup>b</sup>Time course of the degradation shown in Supplementary Figure 3.

1 **FIG 1** | The unrooted circular neighbor-joining tree indicating phylogenetic positions of polypeptide  
2 sequences of Los Rueldos esterases. Positioning is referred to homologous proteins with  
3 unambiguous categorization into lipase/esterase families (from Family I to XIV) according to  
4 Arpigny and Jaeger and further classifications (Arpigny and Jaeger, 1999; Rao et al., 2013).  
5 Abbreviations, as follows: GS-F, Genome Sequences assigned to an esterase/lipase Family (in bold  
6 letters). Sequences from Los Rueldos that correspond to proteins that could not be produced as  
7 soluble active proteins using Ek/LIC 46 vector and *E. coli* strain BL21 (DE3) as a host are indicated  
8 in grey color, while those being active and soluble are indicated in bold.

9 **FIG 2** | pH and thermal profiles of the purified enzymes. The data represent the relative percentages  
10 (%) of specific activity (U/g), in triplicates, compared with the maximum activity using *pNPC*<sub>3</sub> as  
11 substrate. For raw data see **Supplementary Table 1**.

12 **FIG 3** | The thermal denaturation curve of Est<sub>A5</sub> (filled circle) and Est<sub>A6</sub> (open circle) at pH 7.0. The  
13 datasets were obtained by measuring the ellipticity changes at 220 nm obtained at different  
14 temperatures. For raw data see **Supplementary Table 2**.

15 **FIG 4** | 3D comparison of the Est<sub>A5</sub> and Est<sub>A6</sub> hydrolases (A). Zoom into the region that is different  
16 between both proteins, where the possible interaction of Cys152 and Cys181 in Est<sub>A6</sub> can be seen in  
17 panel B. As shown, position 152 is occupied by Arg in Est<sub>A5</sub> instead. Figure has been created using  
18 PMOL(TM) 2.2.3.